Stony Brook University

Assessing the Role of Amyloid Beta in Alzheimer's Disease Using the 5XFAD and TgSwDI Transgenic Mouse Strains

A Dissertation Presented

by

WenJin Xu

to

The Graduate School

in Partial Fulfillment of the

Requirements

for the Degree of

Doctor of Philsophy

in

Biopsychology

Stony Brook University

August 2011

Stony Brook University

The Graduate School

WenJin Xu

We, the dissertation committee for the above candidate for the

Doctor of Philosophy degree, hereby recommend

acceptance of this dissertation.

Dr. John K. Robinson – Dissertation Advisor
Professor of Biological Psychology, Biological Psychology

Dr. Brenda J. Anderson - Chairperson of Defense
Associate Professor, Biological Psychology

Dr. Anne Moyer
Associate Professor, Social and Health Psychology

Dr. William E. Van Nostrand
Professor of Neurosurgery, Stony Brook University

This dissertation is accepted by the Graduate School

Lawrence Martin
Dean of the Graduate School

Abstract of the Dissertation

Assessing the Role of Amyloid Beta in Alzheimer's Disease Using the 5XFAD and TgSwDI Transgenic Mouse Strains

by

WenJin Xu

Doctor of Philosophy

in

Biopsychology

Stony Brook University

2011

The Amyloid Cascade theory of Alzheimer's disease (AD) states that formation and accumulation of amyloid plaques in the brain leads to deleterious downstream effects such as neurodegeneration and gliosis that ultimately cause behavioral deficits and memory loss. In recent years however, the exact role amyloid beta (Aβ) plays in AD has come into question. The most prevalent theory is that amyloid plaque deposition in the parenchyma is the main contributor of pathology in AD. More recent hypotheses state that Aβ deposition in the neural microvasculature in the form of cerebral amyloid angiopathy (CAA) plays a central role in AD. The present longitudinal study uses two transgenic mouse strains with distinctive genotypes, the 5XFAD and TgSwDI, to assess the relationship between location of Aβ deposition and resulting behavioral consequences at 3 and 6 months of age. Behavioral tests were used to assess aspects of spatial working memory as well as well as anxiety, activity level, motor coordination and limb strength. ELISA for Aβ was also performed to determine Aβ40 and Aβ42 soluble and insoluble levels. Finally, stereological quantification and area fraction analysis were done to look

at vascular amyloid plaque deposition, total Aβ deposition, and activated microglia in different brain regions. At 3 months of age, the TgSwDI mouse was behaviorally impaired whereas the 5XFAD was not despite much higher levels of Aβ deposition in the parenchyma. At 6 months of age, both groups of transgenic animals had similar deficits. In this age group, Aβ deposition in the 5XFAD accumulated exponentially in the parenchyma while Aβ levels in the TgSwDI were only moderately elevated. These findings suggest that the location of Aβ deposition in the brain plays a major role in the development of downstream behavioral deficits seen in AD and therefore, is a factor that must be considered in the context of the Amyloid Cascade theory.

Table of Contents

List of Figures

List of Tables

List of Abbreviations

Aβ - Amyloid β protein

Aβ40 - Amyloid β protein (short version) that is 40 amino acids long

Aβ42 - Amyloid β protein (long version) that is 42 amino acids long

ACT – Amyloid Cascade Theory

AD – Alzheimer's Disease

ANOVA – Analysis of Variance

APP – Amyloid Precursor Protein

BBB – Blood Brain Barrier

CAA – Cerebral Amyloid Angiopathy

ELISA - Enzyme linked Immunosorbent Assay

LTP – Long-Term Potentiation

M - Means

PS1 – Presinilin 1

PS2 – Presinilin 2

SD – Standard Deviation

SEM – Standard Error of the Mean

WT – Wild-Type

Chapter 1

Theories of Aβ in Alzheimer's Disease

Alzheimer's disease (AD) is a neurodegenerative disorder that is one of the main causes of death and dementia in the elderly population today. It is characterized cognitively by a steadily increasing severity of memory loss and personality changes independent of any motor or sensory deficits. Early symptoms of AD include the benign forgetting of names and places. Progression leads to inability to do simple tasks such as planning daily events and remembering one's own personal history. Finally, in the late stages of AD, individuals are completely unable to remain autonomous and require help with simple daily tasks such as dressing and undressing and eating and cleaning (Alzheimer's Association, n.d.). Physiologically, symptoms of AD were first described by Alois Alzheimer in 1907 and include an accumulation of neurotoxic amyloid plaques in and around the parenchyma of the brain and neurotoxic tau tangles that are characterized, in general, as a breakdown of the microtubule structure of the neurons (Alzheimer, 1907).

While there have been a number of different theories about the ultimate cause of AD, the leading viewpoint for the past two decades has been the Amyloid Cascade Theory (ACT) first described by Hardy and Higgins in 1992 and elaborated upon by Selkoe (1994). Put in its most fundamental terms, the amyloid cascade theory states that an accumulation of an abnormal protein, amyloid beta (Aβ), in the brain leads to a host of downstream effects such as gliosis, neurodegeneration, and tangle pathology, and these, in turn, cause the observed cognitive and behavioral deficits seen in AD. Perhaps due to its focus on a singular, highly testable cause for AD, the ACT has been thoroughly investigated from a number of different perspectives. Unfortunately, to date, there has not been a clearly supported and replicable finding regarding the

definitive role of Aβ in AD. Instead, a number of viewpoints have surfaced, each pointing to a different form or factor related to Aβ that is implicated as the main culprit in AD.

While a number of different considerations are been taken into account when looking at the involvement of Aβ in AD, they can generally be characterized into two different categories (Figure 1). The first focuses on the involvement of different species and different conformational forms of Aβ on AD. These include the importance of Aβ40/42 ratio on the disease (Younkin, 1998) as well as a viewpoint that is quickly gaining strength and support among the AD research community in recent years; the role of Aβ oligomers in the disorder (Walsh & Selkoe, 2007; Walsh et al., 2002). The second category focuses not so heavily on the type of Aβ that is pathological in AD, but rather where Aβ is deposited. Here, three specific areas are considered. The first is Aβ deposition in the parenchyma (Thal, Griffin, Braak 2008). The second is deposition in the cerebral microvasculature, also known as cerebral amyloid angiopathy (CAA) (Haglund, Kalaria, Slade, Englund, 2006; Kumar-Singh, 2008; Nicoll et al., 2004; Wilcock & Colton, 2009). The third is deposition in the intracellular space (Oakley et al., 2006; Oddo et al., 2006). While the current study focuses on comparing and contrasting the involvement of parenchymal Aβ versus CAA in AD, a brief overview of each of the other viewpoints regarding Aβ is discussed, including a few examples of strengths and weaknesses of each. The parenchymal Aβ deposition and CAA viewpoints are covered last and a discussion of the integration of these viewpoints is also presented.

Aβ42/Aβ40 ratio.

While the initial observation of amyloid plaques in postmortem AD brains implicated their role in the disease, recent genetic advances elucidating the role of amyloid precursor protein (APP) and presenilin (PS1, PS2) mutations in the early, familial form of AD have focused the ACT

away from the presumed pathological and more fibrillar Aβ42 species and more towards a consideration of the balance between the different forms of Aβ. Though the spontaneous form of AD accounts for about 90% to 95% of those affected in the general population, the early onset, or familial form of AD (FAD) is still responsible for the remaining 5%-10%. This form of AD has been linked to a strong genetic component and as such, a multitude of transgenic rodent models have been developed to test the effects of identified PS1, PS2, and APP gene mutations. The PS1 and PS2 mutations are implicated as being integral in the function of the γ-secretase processing of APP. Meanwhile the familial mutations of the gene coding for APP differentially effect processing of the resulting protein. PS1 and PS2 mutations act primarily to increase levels of Aβ42 that is processed from APP (Pimplikar, 2009; Shen & Kelleher III, 2007). The APP mutations can have a variety of effects, ranging from increasing overall Aβ production (Swedish), to increasing Aβ42 versus Aβ40 levels (Florida, London), to creating mutant forms of Aβ (Dutch, Iowa) that are more prone to fibrillization and deposition in certain brain regions (Duff, 1997; Goate et al., 1991; Levy-Lahad et al., 1995; Sherrington et al., 1995). The effect of these identified transgenes has lead to the view that it is not the total levels of Aβ40 or Aβ42 but rather the high proportion of Aβ42/Aβ40 in the brain that leads to downstream effects and cognitive dysfunction. Indeed, reports have shown that while Aβ42 levels are a moderate predictor of AD pathology, the ratio of Aβ42/Aβ40 is a more reliable measure (Lewczuk et al., 2004). In addition, levels of different Aβ species relative to totals have been used to differentiate AD from other senile dementias (Wiltfang et al., 2002). Yet, the picture here is not entirely clear. Transgenic mouse models carrying PS1 and APP mutations have also shown an opposite effect of elevation of Aβ40 to Aβ42 that predicts cognitive and behavioral changes related to AD and the interactions between the two forms of Aβ uncertain (Davis et al., 2004; Herzig et al., 2006;

McGowan et al., 2005) Therefore, while the proportion of the different forms of Aβ species may play an active role in AD pathology, the direction of this effect is certainly still up for debate and in fact, the role of both Aβ42 and Aβ40 in AD may simply be one piece of much larger and more complex picture.

Aβ oligomers.

A recent viewpoint elucidating Aβ involvement in AD partially stems from an unclear numerical relationship between fibrillary amyloid plaque density in the brain and resulting pathology (Pimplikar, 2009; Walsh & Selkoe, 2007). As such, many different forms of Aβ have been investigated in the hopes of finding a better correlate for pathological observations and cognitive decline seen in AD. One of the forms that shows promise in a number of studies is soluble Aβ. More specifically, a number of reports have demonstrated that soluble Aβ oligomers have a much better correlation with synapse loss and other signs of neurodegeneration compared with fibrillar Aβ plaques (Lue et al., 1999; McLean et al., 1999). Due to these observations, it has recently been proposed that the higher order soluble aggregates of Aβ may be the pathogenic species responsible for downstream consequences seen in AD. In addition to being a good predictor of AD pathology, Aβ oligomers have also been shown in a variety of contexts, to inhibit learning and memory processes. For instances, Aβ oligomers injected into the rat have been shown to inhibit long-term potentiation (LTP) in hippocampal cells, a process that is crucial to learning and memory (Shankar et al., 2008; Walsh et al., 2002). In addition, the Tg2576 transgenic mouse models of AD has been shown to exhibit build-up of higher order Aβ oligomers much earlier in development than Aβ plaques, a change that is better correlated with the onset of behavioral changes in these animals (Lesne et al., 2006). However, while the Aβ oligomer hypothesis continues to garner attention, there are still a number of unanswered

questions regarding this viewpoint that need to be addressed. One crucial observation that has yet to be fully discussed is that Aβ oligomers species come in a variety of sizes and forms. It has been reported that Aβ dimers, Aβ–derived diffusible ligands which are soluble globular oligomers of varying sizes of Aβ proteins, and protofibrils, which appear to be an intermediate form of Aβ that can both progress to fibrillize or diffuse into oligomers, are all toxic to hippocampal neurons and can affect processes involved in learning and memory such as LTP and LDP (Harper, Wong, Lieber, Lansbury, 1997; Harper, Wong, Lieber, Langsbury, 1999; Klein, 2002; Shankar et al., 2008; Walsh et al., 1997). Due to this, a second point of contention concerning the instability of Aβ oligomers and the high percentage of experimental artifacts has also been raised. Because Aβ oligomers are metastable and exist in a heterogenous state of monomers, oligomers, and fibrils, variations in *in vitro* and *in vivo* approaches can both significantly alter the composition of extracted and synthesized proteins (Bitan, Fradinger, Spring, Teplow, 2005; Teplow et al., 2006). Therefore, it is often unclear which oligomeric species is being introduced into animals *in vivo* and which type is present and active in AD. Until these questions can be definitively addressed, the viewpoint that the oligomeric form of Aβ is the responsible toxic species in AD remains a work in progress.

Intraneuronal Aβ.

While much of the focus of the amyloid cascade theory has been on the deposition of Aβ in the extracellular space, more and more evidence has begun to suggest that intraneuronal Aβ is a key factor in the accumulation of amyloid plaques in the brain (reviewed in Bayer et al., 2001). In particular, there appears to be a delicate balance between intraneuronal and extracellular Aβ levels that suggests that accumulation starts within the neurons and subsequently develops extracellularly (Oddo, Caccamo, Smith, Green, LaFerla 2006; Svoronsky,

Doms, Lee, 1998; Wilson, Doms, Lee, 1999;). There are a number of observations to support this claim. Reports have shown that in a number of mouse models, intraneuronal build-up of Aβ precedes extracellular accumulation of plaque deposits and that this deposition is much better correlated temporally, with the onset of behavioral deficits seen in these animals (Oakley et al., 2006; Wirths et al., 2001). Furthermore, in a recent immunotherapy study on transgenic mice, extracellular plaque deposition appeared to be cleared before intracellular pools of Aβ and reappearance of Aβ occurred first within intracellular compartments before later spreading to the parenchyma after the conclusion of treatment (Oddo et al., 2006). Yet one of the main arguments against the intraneuronal deposition, indeed, even the mere presence of intraneuronal Aβ in AD is the fact that it has never been reliably detected *in vivo* in AD patients. The nature of intraneuronal Aβ as a proposed initiating factor in Aβ deposition necessarily means that this accumulation occurs very early on in the disease and presumably spreads into the extracellular space by later stages. This means that at autopsy, often there is no chance to visualize intracellular Aβ. As a result, studies looking at this type of deposition has occurred mainly *in vitro* in cultured neurons or in transgenic mouse models where it is unclear whether the intracellular accumulation of Aβ is a natural phenomenon, or a result of the different transgenes and/or promoter types that are used (Duyckaerts, Delatour, Potier, 2009).

Parenchymal fibrillary Aβ.

At its inception, the amyloid cascade theory initially predicted that it was the extracellular fibrillar form of amyloid created by the aggregation of Aβ40 and Aβ42 peptide species that was the primary pathological type of the abnormal protein implicated in AD. This was the original observation made by Alois Alzheimer in postmortem brains when the disease was first diagnosed (Alzheimer, 1907). Early reports demonstrated that total Aβ load in the brain increased with age

and is inversely correlated with performance on a number of learning tasks (Duff 1997; Hsiao & Ashe, 2001). In addition, amyloid plaque accumulation had often been seen to develop in an inside-out manner anatomically, starting at the subiculum and hippocampus and spreading to areas of the neocortex. This was a pattern of deposition that predicted behavioral deficits well since these same brain areas had been implicated in learning and memory processes (Pearson, Esiri, Hiorns, Wilcock, Powell, 1985; Rogers & Morrison, 1985). However, while early findings supported this notion, later observations uncovered alarming inconsistencies. While some studies reported strong correlations between cognitive deficits and Aβ plaque density in the brain, others found no relationship between the two factors (Cummings & Cotman, 1995; Terry et al., 1991). Furthermore, evidence now being uncovered with new PET imaging techniques capable of detecting and looking at Aβ deposition in functional brain images has found that otherwise normal individuals sometimes exhibit large amounts of plaque density in their brains. This has led to the assertion that Aβ build-up does not necessarily correlate with cognitive decline (Nordberg, 2004; Sair, Doraiswamy, Petrella, 2004; Villemagne et al., 2008). Finally, new developments in immunization against amyloid plaques successful in clearing plaque deposition from the brain has recently been shown to have very modest effects at rescuing cognitive deficits in human patients although initial trials in transgenic mice produced beneficial results. This suggests that there are possible other factors involved in the cognitive decline of patients with AD unrelated to amyloid plaque density that remain a mystery (Lemere & Masliah, 2010; Morgan et al., 2000).

Microvascular associated amyloid (Cerebral Amyloid Angiopathy).

Defined most simply as the accumulation of amyloid protein in the microvasculature of the brain, cerebral amyloid angiopathy (CAA) is a condition that has long been known to co-occur

with AD (Smith & Greenberg 2009). While there are many different types of possible vascular Aβ accumulation, by far the most common, and the type most closely associated with AD, is Aβ CAA or accumulation of the Aβ type. CAA's role in AD related dementia stems from a number of different observations. First, and one of the most striking, is the prevalence of CAA among AD patients. Compared to non-demented controls, the prevalence of CAA is almost 3 times higher in the AD population (Yamada, 2002). Second, CAA can itself be a cause of dementia in the aging population. Accumulation of Aβ in the microvasculature has been shown to cause degradation of the blood brain barrier (BBB), decreased blood flow, destruction of smooth muscle cells along the vessel walls, micro-hemorrhaging and even ischemia in severe cases (Stopa et al., 2008; Thal et al., 2009; Vinters, Wang, Secor, 1996). As might be predicted then, when these two dementias are compounded, AD patients with co-occurring CAA often experience a more severe form of the disorder that leads to accelerated cognitive decline compared to those with AD alone (Pfeifer et al., 2002a). Third, many studies have shown the critical role that the cerebral microvasculature plays in the system that regulates the balance between Aβ production and elimination in the brain. It is thought that when amyloid plaque accumulation damages the microvasculature, this system fails to function properly, leading to a failure in elimination and resulting accumulation of Aβ in the parenchyma as pathological plaques (Nicoll et al., 2004; Wilcock & Colton, 2009). Fourth, there is some evidence that raises the possibility of Aβ being generated directly by smooth muscle cells. Microvessel extracts from AD patients have been shown to include Aβ and *in vitro* experiments have demonstrated smooth muscle cells as being capable of producing APP and Aβ (Kawai et al., 1993; Maness et al., 1994; Rensink, de Waal, Kremer, Verbeek, 2003).

Though CAA pathology has been clearly established as being similar to and perhaps complimentary with AD pathology, a number of the mechanisms seen in both the accumulation and type of Aβ leaves a lot to be explained. One critical difference is the finding that while Aβ42 appears to be the main pathological and fibrillary species in AD, it is the traditionally non-fibrillar Aβ40 peptide that comprises the majority of deposition in CAA (Castellani et al., 2004). In addition, one of the issues that questions the parenchymal fibrillary Aβ viewpoint can similarly be leveled against the CAA argument. Namely, CAA has been found in non-demented individuals and in many of those cases, has no effect on cognitive function (Castellani et al., 2004). Therefore, although it is clear that CAA likely plays a role in AD-related dementia, the mechanisms that cause CAA to develop into or complement AD pathology is still not entirely clear.

Parenchymal fibrillary Aβ deposition and CAA.

While the parenchymal fibrillary Aβ and CAA viewpoints both have their strengths and weaknesses, there now appears to be a position that integrates both. A number of recent reports have suggested the idea that AD characterized solely by parenchymal deposition of Aβ on the one hand and solely by CAA on the other, are in fact at opposite ends of a spectrum of dementia-related disorders caused by abnormal Aβ deposition in the brain. This combination of both types of symptoms has recently been identified as mixed dementia and presumably lies somewhere in the middle of that spectrum (Gold et al., 2007; Jellinger & Attems, 2007; Thal, Griffin, Braak, 2008). That the ApoE ε4 allele that has been known to predispose individuals to AD and cause earlier onset and more severe cognitive decline, has also been linked to CAA type 1 (deposition in capillaries) further speaks to the integration of these two types of dementia (Strittmatter et al., 1993; Thal et al., 2008). In addition, the results of immunotherapy demonstrate a dynamic

continuation between Aβ deposition and clearance through the microvasculature, such that immunotherapy, which relieves Aβ plaque deposits in the parenchyma, presumably overloads the clearance system and leads to increased severity of CAA in animal models (Pfeifer et al., 2002b). Finally, symptoms of CAA including vascular occlusion and lesions have been demonstrated to be good predictors of cognitive dysfunction in the early stages of AD, but become less useful at identifying later stages, suggesting a continuum of progression initiated by CAA but leading to and increasing in severity with parenchymal deposition of Aβ (Jellinger & Attems, 2007).

Chapter 2

Transgenic Mouse Models

The identification of mutations in the APP, PS1 and PS2 genes implicated in familial AD (FAD) as well as CAA has allowed the creation of numerous transgenic mouse models of these disorders. What follows is a review of the two main mouse models used in the present study, the 5XFAD and TgSwDI animals. One point that is important to note here is that these animals are not models AD, but rather the effects of parenchymal Aβ deposition and CAA on AD respectively. To treat them as models of the disorder would inevitably see them falter on a number of different levels. However, as representations of certain aspects of the pathology seen in AD, they are invaluable tools for researchers.

5XFAD mouse.

While there have been a number of different mouse models of AD that showcase Aβ plaque deposition as the main pathological species in the brain, perhaps none is more effective at producing an early and robust effect than the recently developed 5XFAD mouse (for reviews of mouse models of AD, see Duyckaerts, Potier, & Delatour, 2008; Elder, Gama Sosa, & Gasperi, 2010; Guenette & Tanzi 1999). Originally created and reported upon in 2006, this novel model of amyloid pathology contains 3 APP mutations (APP K670N/M671L [Swedish], I716V [Florida], V717I [London]) and 2 presenilin mutations (PS1 M146L, L286V) on a B6/SJL background under a Thy1 promoter (Oakley et al., 2006). As a result, it rapidly produces an excess of both the Aβ40 and Aβ42 proteins at a very early age. Due to the presence of the APP London and Florida mutations as well as the presinilin mutations, the ratio of Aβ42 to Aβ40 is shifted so that a much higher percentage of the former is produced than the latter in these animals (Elser & Wolfe, 2001). Compared to the often used Tg2576 mouse, Aβ plaque

accumulation in the 5XFAD begins at 3 months of age and accelerates at an exponential rate as the animal ages and by 12 and 16 months, the 5XFAD have Aβ levels 4-fold higher than their counterparts (Oakley et al., 2006; Ohno et al., 2007). In addition, the 5XFAD demonstrates Aβ related pathology that did not appear to be present in previous strains of mice such as neurodegeneration, microglial and astroglial activation, as well as intraneuronal Aβ accumulation (Oakley et al., 2006).

Histologically, the 5XFAD mouse is characterized by a build-up of diffuse and fibrillary Aβ42 in the deep cortex and subiculum starting at 2 months of age and spreading rapidly to hippocampus through 4 and 6 months. By the 9-month time point, Aβ42 plaque deposition is widespread throughout all areas of the brain including thalamus and cortex. Meanwhile, Aβ40 accumulation in these animals begins at about 3 months of age and consistently deposits at a much slower rate than Aβ42 throughout development (Oakley et al., 2006). In addition to the massive amount of plaque pathology present in these animals, the 5XFAD is one of the first models to demonstrate an accumulation of Aβ42 intraneuronally, suggesting the possibility that aggregation of the abnormal protein within the cell precedes extracellular plaque build-up. Furthermore, the 5XFAD mouse has been observed to exhibit microglial and astroglial activation and subsequent neuroinflammation accompanying Aβ deposition in the same brain areas, a phenomenon that had been missing in a number of previous murine models. Finally, unlike a number of predecessors, neurodegeneration in cortical layer 1 and 5 have been reported in this animal and also appear to be associated with the presence of Aβ42 in associated brain areas (Oakley et al., 2006; Ohno et al., 2007).

Behaviorally, the 5XFAD has been shown to be impaired in hippocampal dependent memory tasks such as the Y-maze spontaneous alternation and contextual and trace fear

conditioning tasks at 6 and 14 months of age (Kaczorowski, Sametsky, Shah, Vassar, Disterhoft, 2009; Kimura, Devi & Ohno, 2010; Kimura & Ohno, 2009; Ohno, 2009; Ohno et al., 2007). In addition, one group has reported the presence of a peculiar motor phenotype where 5XFAD mice exhibit balance and limb strength deficits in addition to reduced body weight and anxiety levels starting at the 9 month time point which coincides with very high levels of Aβ42 accumulation (Jawhar, Trawicka, Jenneckens, Bayer, Wirths, 2010). This observation has also been linked to the presence of Aβ42 in the spinal cord of these animals that appear to cause significant axonal degeneration.

Due to its histological, pathological, and behavioral characteristics, the 5XFAD mouse is a great candidate model to illustrate the involvement of parenchymal fibrillary accumulation of Aβ42 in AD. These mice exhibit plaque deposition early on in development with associated neuronal pathologies and cognitive memory dysfunction. Furthermore, because of the early and rapid deposition of Aβ, the 5XFAD allows researchers a opportunity to investigate the overall effect of accumulating levels of Aβ and associated deficits through a long period of development.

TgSwDI mouse.

First developed and reported on in 2004, the TgSwDI mouse is a unique animal model of Aβ deposition in that it does not produce high amounts of Aβ40 or Aβ42 compared to other transgenics, yet exhibits an accumulation rate comparable to other strains producing higher overall levels of Aβ. (Davis et al., 2004; Davis et al., 2006). Genetically modified to express the Swedish (K670/M671L), Dutch (ESQQ), and Iowa (D23N) mutations on a C57Bl/6 background with a Thy 1.2 promoter, the TgSwDI produces large amounts of a mutated form of Aβ40 that has been shown to be prone to fibrillization and accumulation in the cerebral microvasculature

which in turn, leads to vascular pathologies (Levy et al., 1990; Van Broeckhoven et al., 1990; Van Nostrand et al., 2001; Xu et al., 2008).

Histologically, the TgSwDI mouse is characterized by early distribution and accumulation of fibrillar Aβ deposits in the cerebral vasculature around the thalamus and subiculum beginning at 3 months of age that is accompanied by neuroinflammation, activation of astroglia and microglia, and cell death around these areas. Compared to the 5XFAD which overexpresses human APP, leading to rapid accumulation of Aβ in the brain parenchyma, the TgSwDI produces very low levels of mutated human APP throughout its life span. Due to this, very low levels of Aβ40 and Aβ42 are detected in these mice compared to other transgenic models. However, despite this underproduction, accumulation of both soluble and insoluble Aβ (with a skew towards the Aβ40 versus Aβ42 species) can be seen in the brain parenchyma of these animals starting at 3 months and steadily increasing to 12 months of age. These Aβ aggregations have been reported to be mainly of the diffuse rather than fibrillar variety, and first appear in the subiculum, hippocampus, and cortex, and spread to the olfactory bulbs, thalamus, and finally the majority of the forebrain area by 12 months. It is hypothesized that Aβ build-up in these areas despite low expression of human APP in the TgSwDI may be due to two main factors. The first involves the rapid deposition of Aβ in the brain microvasculature and subsequent inhibition of transport of the protein through the blood brain barrier and out of cortical areas (Davis et al., 2004; Davis et al., 2006; Vasilevko, Xu, Previti, Van Nostrand, Cribbs, 2007; Xu et al., 2007;). The second is the possibility that due to the Dutch and Iowa mutations present in these animals, the Aβ produced is of a mutated variety that has been shown to be more conducive to fibrilization than normal wild-type amyloid (Davis & Van Nostrand, 1996; Miravalle et al., 2000; Van Nostrand et al., 2001).

While very little work has been done characterizing the TgSwDI mouse behaviorally, initial reports show that compared to the 5XFAD mouse, it shows no signs of any motor, coordination, or anxiety changes. However, Barnes maze testing to evaluate aspects of spatial working memory reveal that TgSwDI mice are impaired in learning the position of the box at the 3, 9, and 12-month time points. Interestingly, these behavioral deficits appear in close temporal proximity to cerebral vascular Aβ deposition in these animals, suggesting a possible relationship between the two observations (Xu et al., 2007).

In summary, the TgSwDI is a good model of CAA due to the unique pattern of its Aβ deposition. Aβ associated with cerebral microvessels are detectable at 3 months of age and increase in number and area of deposition through 6, 9, and 12 months. In addition, pathologies associated with CAA are also detected in these animals at older time points. Finally, behavioral deficits correlated with the onset of Aβ deposition can be seen in both young and aged transgenics.

Chapter 3

Aims

The current study seeks to evaluate the roles that parenchymal Aβ plaque deposition and CAA play in AD pathology using the 5XFAD and TgSwDI mouse models respectively. While previous research has shown that both of these mouse models demonstrate impaired cognitive functioning at later stages in development, to date, no one has studied whether these impairments precede or follow the deposition of Aβ in the parenchyma or more closely follow CAA. To develop a clearer understanding of the relationship between functional deficits and pathology, we conducted a strain comparison between the 5XFAD and TgSwDI through different stages of maturation specifically looking at how behavioral deficits correlated with pathological phenotypes. The present study sought to:

Compare the 5XFAD and TgSwDI on onset and accumulation of parenchymal amyloid at 3 and 6 months of age.

Compare the 5XFAD and TgSwDI on CAA pathology at 3 and 6 months of age.

Compare the 5XFAD and TgSwDI on Aβ40 and Aβ42 soluble and insoluble species' levels at 3 and 6 months of age.

Compare the 5XFAD and TgSwDI on a behavioral battery that assessed aspects of spatial working memory, motor coordination, anxiety, limb strength, and overall activity level at 3 and 6 months of age.

Determine the role that parenchymal amyloid and CAA pathology play in observed behavioral deficits that develop at 3 and 6 months of age in the 5XFAD and TgSwDI.

Rationale

The ACT has been a major organizing theory behind AD research in the past 2 decades. It makes the broad prediction that Aβ is the main cause of AD and associated cognitive deficits. However, due to its high testability, numerous inconsistent findings regarding the specific role of Aβ in AD has emerged. These findings challenge not only the importance of absolute Aβ levels in the brain, but also raise issues regarding different forms of Aβ and where the pathological protein is deposited in the brain and how these factors effect AD and associated cognitive symptoms (Pimplikar, 2009). Considering the emergence of recent immunological studies aiming to eliminate Aβ from the brain parenchyma as a possible treatment for AD (Lemere & Masliah, 2010; Morgan et al., 2000) and the comorbidity of CAA with AD (Yamada, 2002), the effect of deposition of Aβ in the parenchyma and cerebral microvasculature surfaces as an important addendum to the ACT that is crucial to investigate because of the possible contributions to the development of targeted clinical treatments of Aβ in an effort to relieve symptoms of AD. Yet, absolute levels of the different species of Aβ, and more specifically, the pathological Aβ42 and more benign Aβ40 (Selkoe, 1994; Younkin, 1998) must also be assessed to determine how the quantity of Aβ species interacts with its spatial deposition to lead to AD-like cognitive changes. In order to do so, the present study chose to use the 5XFAD and TgSwDI mouse models of Aβ pathology and compare them through 2 developmental age points. These animals allowed us not only to assess the spatial deposition of Aβ but also the different levels of Aβ species and how these factors related to AD-like cognitive change.

The 5XFAD and TgSwDI animals were used in the present study to represent parenchymal deposition of Aβ and CAA respectively while at the same time providing differential accumulation levels of Aβ42 and Aβ40 through development. The 5XFAD murine model was used specifically because it demonstrates one of the most robust parenchymal

amyloid phenotypes of any transgenic murine model of Aβ to date. Compared to the benchmark Tg2576, the 5XFAD generates higher levels of Aβ42 at an earlier rate (Oakley et al., 2006) and deposits amyloid primarily in the parenchyma. This phenotype allowed us to study the effect of highly elevated levels of Aβ, deposited within the parenchyma, in a short developmental time period in these animals. In contrast, the TgSwDI is the only known murine model of Aβ accumulation and deposition as CAA to date (Davis et al., 2004). In addition, the TgSwDI does not produce highly elevated levels of any species of Aβ and compared to the 5XFAD, generates larger amounts of Aβ40 than Aβ42. If considered together, these two murine models allowed us the unique opportunity compare the differential effects of parenchymal and CAA Aβ deposition and also assess the effects of highly contrasting levels of Aβ species accumulation through two developmental time points.

Although the use of the 5XFAD and TgSwDI murine models to represent the differential deposition and accumulation of Aβ in the present study was a clear decision given the unique phenotype expressed by each animal, the use of the Barnes maze to assess spatial working memory was a more deliberate decision. To date, a number of different apparatus' have been used with murine models in AD research as a way of evaluating spatial working memory. These range from the Morris water maze, to the T-maze, and the radial arm-maze. However, for the present study, we wanted a robust spatial working memory measure that did not include an appetitive or particularly aversive motivator due to the potential for associated confounds. This left the Barnes maze as the best choice due to its reliance on the rodent's inherent fear of open and brightly lit spaces as the main motivators for escape (Barnes, 1979). To further ensure that the Barnes maze measures were not influenced by non-cognitive factors, a behavioral battery

was used to assess different aspects of anxiety, activity level, and motor strength and coordination in order to attempt to rule out these potential confounds in the present study.

Due to the use of the 5XFAD and TgSwDI murine models as representations of parenchymal and CAA Aβ depositions, the regions of interest (ROI) that we chose to observe with respect to Aβ accumulation were the subiculum, thalamus, and cortex. These were chosen based on previous reports on the 5XFAD and TgSwDI that identified the subiculum as where amyloid deposition first appeared and the thalamus and cortex as subsequent areas of deposition (Davis et al., 2004; Xu et al., 2007; Oakley et al., 2006).

In summary, the inconsistencies in the ACT coupled with emerging immunotherapy methods for treating AD provided the rational for conducting a study that sought to assess the contributions of the effects of spatial deposition and accumulation of Aβ, whether in the parenchyma or as CAA, on cognitive change. In order to do so, the 5XFAD and TgSwDI murine models were used because they were judged to represent most robustly, the accumulation of Aβ in the aforementioned areas. In addition, the differential Aβ42 and Aβ40 accumulation rates in these animals allowed for the opportunity to evaluate how each contributed to cognitive dysfunction through development. Finally, the Barnes maze was used to assess spatial working memory because it did not employ an appetitive or particularly aversively motivated stimuli that may have otherwise allowed for undesirable confounds to influence these measures.

Chapter 4

Subjects

Three groups of mice (TgSwDI, 5XFAD, and WT) at each age (3 and 6 months) were used for this study. In the 3-month age group, there were seven TgSwDI (2 female, 5 male), six 5XFAD (6 male), and five WT (5 male) mice for a total of 18 animals. In the 6-month age group, there were six TgSwDI (4 female, 2 male), seven 5XFAD (4 female, 3 male), and eight (3 female, 5 male) WT mice for a total of 21 animals. All TgSwDI animals used in the present study were heterozygous for the human Swedish/Dutch/Iowa APP transgene. All 5XFAD animals were heterozygous for the APP and PS1 transgenes present.

Procedure

Behavioral testing.

Animals in the 3 and 6-month time periods were tested using the same procedure and progression of tasks. Testing took place through the span of 2 weeks. During the first week, animals were tested on days 1, 3, and 5. Digiscan and Light/Dark box were done back to back on day 1. Wire Hang and Roto-rod were done back to back on day 3. 0-maze was done on day 5 and animals were weighed afterwards. During the second week, animals were tested on the Barnes Circular maze on days 1-5. After the second week of testing, animals were perfused and immunohistochemistry was performed on the brain tissue.

Immunochemical and immunohistochemical analysis.

Part 1 (ELISA):

Brains of all 3 groups of animals (TgSwDI, 5XFAD, WT) at each time point were analyzed for the soluble and insoluble forms of Aβ40, Aβ42, and total Aβ using ELISA. Animals displaying no Aβ burden in these analyses were excluded from the second part of the assessment.

Part 2 (immunohistochemical analysis)

The brains of WT animals did not display any amyloid pathology as assessed by ELISA, so were not analyzed further. Sagittal brain sections of the 5XFAD and TgSwDI mice that had the lowest, middle, and highest measures on ELISA for total amyloid were stained for fibrillary amyloid in the parenchyma and microvasculature, total amyloid burden, and activated microglia. Specifically, the subiculum, cortex, and thalamus were inspected with respect to each of the immunohistochemical analysis. These regions were selected due to previous findings in 5XFAD and TgSwDI mice that suggest that amyloid deposition first appears in these areas (Oakley et al., 2006; Xu et al., 2007). A count and percentage of microvessels associated with Aβ plaques was taken. In addition, area fraction analysis was done to assess total amyloid burden and density analysis was done to assess activated microglia.

Behavioral Testing

Barnes circular maze.

The circular platform used in the current study was an adaptation of the Barnes Maze apparatus originally developed for rats (Barnes, 1979). It consisted of a wooden disk with 8 escape holes along the edge spaced equally apart and numbered from 1-8. Shelves were built under the holes such that an escape box could be placed under the holes. The escape boxes were designed so that they could easily be attached and removed upon entry of the mouse. The disk measured 91cm in diameter while the escape holes were 5cm in diameter. They were spaced 24.5cm apart. The escape box measures 10cm x 8.5 cm x 4cm.

The circular maze platform was placed at one end of a large room and elevated 75cm off the. Each mouse was given 2 trials per day separated by a 15 minutes intertribal interval. Testing lasted a total of 5 consecutive days. An observer sat 1.5m away from the maze during trials.

Visible distal cues were placed around the room and stayed constant throughout testing. At the start of each trial, each mouse was picked up from their home cages by the base of their tail and placed onto the center of the maze. The mouse was allowed a maximum of 5 minutes to find its assigned hole and escape box. When the mouse entered the box, the timer was stopped and they were given 1 minute inside the box before being transferred back to the home cage. If the mouse did not find the escape hole within the 5 minute limit, they were picked up by the base of their tail and placed into the hole and left there for 1 minute. During the trial, the time it took the mice to find the escape box (latency to find) and the time it took them to enter into it (latency to enter) was recorded. In addition the number of errors that were made before finding the escape hole was noted (errors). An error was defined as a nose poke into a hole that did not have an escape box under it.

Wire hang.

The wire hang apparatus consisted of a 44cm long stainless steel wire suspended 54cm off the ground by two wooden posts. At the beginning of each trial, mice were placed on the wire so that only their front paws contact the wire. A timer was then started and the amount of time mice were able to hang onto the wire before they fell onto a foam pad below the apparatus was recorded. If mice hung on for one minute, they were taken off the wire and given the maximum hang time of one minute. If they were able to crawl along the wire to one of the wooden posts they were also given the maximum hang time. Each mouse underwent three consecutive trials during testing.

Rotarod.

The Rotarod apparatus (Medical Associates Incorporated [model ENV-575M] is a mechanized 30cm long rod divided into five 6cm sections by 4 plastic white discs. The speed of rotation

increased from 4rpm to 40rpm through the course of five minutes. Mice were run 4 at a time on the different sections of the rod. At the start of each trial, mice were placed on the rod.. Time that it takes each mouse to fall off the apparatus was recorded along with the corresponding speed at that time. Each mouse was tested for three consecutive trials and each trial ended when all mice had fallen off the rod.

0-maze.

The circular 0-maze used in the current study consists of a circular ring 58cm in diameter and 6.5cm wide elevated to a height of 61cm. The circular ring is divided into 4 equal quadrants 14.5cm in length, 2 that were bordered by 26cm walls of plexi-glass and 2 that were exposed without any borders.

Each mouse underwent one trial per day for 2 days. Each trial consisted of a 5 min time interval where mice were placed onto the circular 0-maze at the border between an open and closed quadrant and allowed to explore the maze. The time mice spent in each of the open and closed quadrants was recorded. At the end of 5 minutes, mice were removed from the maze and a 75% ethanol solution was used to clean the platform.

Light-dark box.

The light-dark box is a 43cm x 21cm x 21cm plexiglass container divided into two parts. The "dark" part was made of black plexiglass with a cover and was 14cm long while the "light" part was 29cm made with clear plexiglass with no cover. These were separated by a black plexiglass wall with a 5cm x 5cm hole cut into the middle to allow for transitions.

Each mouse received one five minute trial that started by placement into the dark part of the box and with the cover closed. A transition was defined as the mouse passing the entirety of

its body into a different section of the box. The number of transitions, time spent in the light section, and time spent in the dark section, were each recorded.

Digiscan.

The Digiscan container had the same dimensions as the light-dark box and was constructed of clear plexiglass. It recorded ambulation, defined as movement parallel to the floor (ie. walking) and horizontal activity level, defined as all movement (including grooming, rearing activity) over 5 minutes. In addition, the number of assisted and unassisted rearings was recorded. An unassisted rearing was defined as the animal rising on its hind legs without placing its front paws on a wall for support, whereas an assisted rearing was defined as a rearing while placing paws on a wall for support. Since there was no difference in the rearing scores, the assisted and unassisted measures were combined into one rearing measure.

Tissue Preparation

Procedure was adapted from Vasilevko et al. (2007) and Xu et al., (2007). Briefly, mice were overdosed with 2.5% avertin and intracardially perfused with PBS. The cerebellum was cut off and discarded and the brains were removed and bisected along the midsagittal plane. One hemisphere was snap frozen and used for ELISA. The other hemisphere was placed in 70% ethanol, then treated with xylene and embedded in paraffin for immunohistochemical and immunoflourescence evaluation.

Enzyme linked Immunosorbent Assay (ELISA) for Aβ Species

Procedure was adapted from Davis et al. (2004). Sandwich ELISAs were conducted for both soluble and insoluble forms of Aβ40 and Aβ42. Briefly, soluble Aβ40 and Aβ42 levels were determined by specific ELISAs of carbonate-extracted mouse forebrain tissue. Insoluble Aβ40 and Aβ42 were determined by ELISA of guanidine lysates of the insoluble pellets

resulting from the carbonate-extracted brain tissue. The carboxyl terminus-specific antibodies m2G3 and m21F12 were used to capture Aβ40 and Aβ42 respectively and biotinylated antibody m3D6, which is specific for human Aβ was used for detection. Total levels of Aβ40 and Aβ42 were determined by combining the results of each individual measure of soluble and insoluble species of Aβ40 and Aβ42.

Immunohistochemical Analysis

Immunohistochemistry was performed similar to the procedures used in Davies et al., (2004) and Xu et al., (2007). For each hemisphere, a total of 100 sections were cut starting at the most distal region of the thalamus. Paraffin sections were cut in the sagittal plane at 10 μm thickness using a sled microtome. These were then floated on a 45^{o}C water bath and transferred onto glass slides. Each of a total of 50 slide contained 2 sections that were separated by 10 cuts (ie.slide #1 had section #1 and #11, slide #2 had section #2 and #12, slide #3 had section #3 and #13, etc.). Slides were deparaffinized by immersing in xylenes and rehydrated with decreasing concentrations of ethanol. Because previous studies indicated Aβ deposition initially in the subiculum that progresses to the cortex and thalamus (Davis et al., 2004; Oakley et al., 2007; Xu et al., 2007), these same regions were used in the present study.

Antigen retrieval was conducted via 5-minute incubation with protease K for collagen. Rabbit polyclonal antibody to collagen type IV was used for immunohistochemical identification of microvessels. Anti-rabbit donkey IgG 594 counterstain was used for fluorescence imaging. Secondary thioflavin S staining for fibrillary amyloid was then performed as described in Dickson et al., (1990).

Antigen retrieval was conducted via 5-minute incubation with protease K and slides were blocked with .3% Triton X blocking buffer for 15 minutes. For imaging of total Aβ burden,

Rabbit polyclonal 1-28 antibody to amyloid was used. Anti-rabbit IgG 488 counterstain was used for fluorescence imaging.

Imaging of activated microglia was performed as described in Xu et al., (2007). Briefly, anti-keratin 5D4 mouse IgG antibody to microglia was used. A secondary anti-mouse biotinylated antibody was used for antibody retrieval and the slides were developed with stable DAB.

All stereological work was done on an Olympus BX60 microscope attached to a Dell desktop. Pictures were taken with an Olympus DP72 camera attached to the microscope. Percentage microvessels associated with Aβ was assessed using the Stereologer program (Stereologer, Systems Planning and Analysis, VA, USA) and dividing the total microvessels by microvessels associated with Aβ. Here, for each animal that was assessed (3), every tenth section was sampled and 10 sections per reference space was counted for total microvessels and microvessels associated with amyloid for the cortex and thalamus. For the subiculum, every tenth section was sampled but only 4 sections per reference space was counted for total microvessels and microvessels associated with amyloid. To obtain an aggregate measure of percentage microvessels associated with amyloid, the total number of microvessels across all samples for each brain region for each animal was added and divided by the total number of microvessels associated with amyloid across all samples for each brain region. Total amyloid was assessed by measurement of area fraction with the ImageJ version 1.44 program developed by NIH. A total of 10 images for each brain region (cortex, subiculum, and thalamus) was analyzed per animal (3). Images were thresholded twice. The first at 33/255 was used to look at dense core plaque deposition but not spray pattern plaque deposition that was apparent in some animals. The second at 22/255, took into account both dense core plaque deposition as well as

smaller, spray pattern deposition of Aβ. Finally, microglia density was assessed using the stereologer program version 1.3. This procedure was the same as used in Xu et al., (2007).

Statistical Analysis

All data were analyzed using the StatView statistical software. Two-way ANOVAs were first used to test the main effects and interaction between age and genotype on all of the behavioral measures. In addition, one-way between groups ANOVA was used to analyze data from the 0-maze, Light-Dark box, and Digiscan as well as the ELISA for Aβ species. Repeated measures ANOVA was used analyze data in the Wire Hang, Rota-rod, and Barnes maze. These were conducted to further look at the individual differences between animal groups at 3 and 6 months of age. A-prior comparisons between 5XFAD and TgSwDI were done to investigate possible differences between transgenic groups in the Barnes maze latency to find, latency to enter, and error measures. In addition, a regression analysis was used to investigate Barnes maze in order to obtain a singular rate-of-learning measure for each individual animal. Finally, correlations were used to compare behavioral data that was significant with ELISA measures.

Chapter 5

Aggregate Analysis

Behavior.

In order to account for possible motor, anxiety, and activity level derived confounds that might affect the Barnes maze spatial working memory measure, a two-way between groups ANOVA with age and genotype as the between groups measure was done on the non-cognitive battery of behavioral tasks. There was a significant effect of age on the horizontal activity level measure ($F[1,34] = 90.73$, $p<.05$), demonstrating that when genotypes were aggregated, animals were more active at the later 6 month age point. Furthermore, there was a significant main effect of genotype on rearings in the open field ($F[2,34] = 3.86$, $p<.05$), time spent in the dark quadrant of the light/dark box ($F[2,34] = 5.97$, $p<.05$), and transitions in the light dark box ($F[2,34] = 7.81$, $p<.05$). Age was not a significant factor in any of these measures nor was the interaction between genotype and age (data not shown). Finally, there was no significant main effect or interaction in the time spent in the open quadrants of the O-maze (data not shown). Hybrid two-way repeated measures ANOVAs were also done to investigate performance of animals on the rota-rod and wire hang measures. It was found that there was no significant main effect or interaction in the rota-rod (data not shown). However, in the wire hang measure, a main effect of trial was found ($F[2,68] = 3.74$, $p<.05$), demonstrating that animals remained on the wire longer on later trials. As a final measure of activity level, the number of errors made in the Barnes maze was divided by the latency to enter measure on each day to obtain a measure of error rates. A hybrid two-way repeated measure ANOVA done to compare rate of errors revealed that neither genotype nor age had a significant main effect on error rate and there were no significant interactions. Instead, there was a significant main effect of trial on error rate ($F[4,128] = 8.14$,

$p<.05$) demonstrating that error rates generally changed from trial to trial independent of genotype or age. Due to the significant genotype effects present in a number of these tasks, groups of animals at both 3 and 6 months were further analyzed on these non-cognitive tasks with one-way between groups ANOVAs to investigate where these differences were evident.

To investigate possible differences in the Barnes maze spatial memory task, a hybrid two-way repeated measures ANOVA was conducted on latency to find and error measures. There was a significant main effect of genotype ($F[2,33] = 7.30$, $p<.05$) and age ($F[1,33] = 4.86$, $p<.05$), as well as a genotype-age interaction ($F[2,33] = 5.06$, $p<.05$) on the latency to find measure. Furthermore, there was a three way interaction between genotype, age, and trial ($F[8,132] = 2.99$, $p<.05$) on latency to find. This demonstrated that differences in latency to find measures across days were partially contingent on the age and genotype of the mice. Finally, a main effect of trial ($F[4,132] = 11.14$, $p<.05$) illustrated a possible learning effect on latency to find measures. Due to the significance of the main effects present as well as the interactions in latency to find, further one-way between groups ANOVAs were conducted to compare each genotype at 3 and 6-months of age. A hybrid two-way repeated measures ANOVA conducted on errors made in the Barnes maze revealed a significant main effect of age ($F[1,33] = 9.09$, $p<.05$) as well as an effect of trial ($F[4,132] = 20.18$) and a three way interaction between trial, age, and genotype ($F[8,132] = 2.18$, $p<.05$). These results demonstrate that age had a significant effect on errors made and errors decreased across trials. Finally, errors across days were partially contingent on the age and genotype of the mice. Due to the significant main effect and interactions found in the error measures, futher one-way between groups ANOVAs were conducted to compare each genotype at 3 and 6-months of age.

Because there is a possible dissociation between working and reference memory measures in the Barnes maze, latency to find and errors on the two separate trials on each day of Barnes maze testing was analyzed separately in a two-way ANOVA. Here, there are three assumptions that can be made. The first is that the first trial on the first day is not a strict memory measure since no animal has been exposed to the escape position at this point. Second, the first trial of each day may be considered a reference memory measure because of the long inter-trial interval (24 hours). Third, the second trial of each day may be considered an assessment of spatial working memory due to the short inter-trial interval (15 minutes). The two-way ANOVA's conducted for latency to find on each trial of each day revealed a significant effect of genotype on trial 1 of day 2 ($F[2,31] = 4.41$, $p<.05$) as well as on trial 1 of day 3 ($F[2,31] = 4.23$, $p<.05$) and trial 2 of day 3 ($F[2,31] = 7.22$, $p<.05$). There were no other significant main effects or interactions on any trial. These results demonstrate a number of points. The first is that all the animals regardless of age or genotype started off at the same level of performance on latency to find measures, suggesting that all animals had similar activity levels and similar motor capabilities. Second, the significant main effect of genotype on latency to find measures on trial 1 day 2 and trial 1 day 3 suggest that there is a significant difference between the groups in an aspect of reference memory. Fisher's post-hoc comparisons of these trials revealed that 5XFAD ($p<.05$) and TgSwDI ($p<.05$) differed significantly from WT animals on trial 1 day 2 and TgSwDI ($p<.05$) differed significantly from WT animals on trial 1 day 3. Two-way ANOVAs conducted for errors made on each trial of each day of testing in the Barnes maze revealed a significant group/age interaction on trial 1 of day 1 ($F[2,32] = 5.35$, $p<.05$). This shows that errors made during first exposure to the Barnes maze were affected by both genotype and age of the animals. Subsequently, there was a main effect of age on trial 1 ($F[1,32] = 5.09$, $p<.05$) and 2

(F[1,32] = 7.76, p<.05) on day 2, trial 2 (F[1,32] = 13.34, p<.05) on day 3, and trial 1 and 2 on day 4 (F[1,32] = 14.99, p<.05; F[1,32] = 5.16, p<.05) and 5 (F[1,32] = 8.46, p<.05; F[1,32] = 6.79, p<.05). That no other main effects were significant demonstrated that errors on the Barnes maze were influenced by age and furthermore, animals at 6 months of age in general, made more errors than animals at 3 months of age on days 2, 4, and 5.

ELISA.

Since all of the ELISA measures for Aβ species for both the 3 and 6 month age groups were significant except for Aβ40 insoluble (F[1,10] = 3.67, p = *n.s.*) which was trending towards significance at the 3 month time point, a correlation matrix was performed to investigate how strong the relationship of each of the measures was to one another. Table 1 shows that correlation between Aβ species ranged from a high of r=.95 (Aβ40I with Aβ42S) to a low of r=.69 (Aβ40S with Aβ40I).

Aβ Measures and behavior.

The amyloid cascade theory points to the central role that Aβ build-up in the brain plays in the gradually cognitive decline seen in AD. In order to evaluate this theory, a multiple regression was performed where each of the Aβ species was inserted into a model with the Barnes maze latency to find learning measure as the dependent variable. It was found that together, the Aβ42I, Aβ42S, Aβ40I, and Aβ40S species accounted for 9.9% of the variance observed in latency to find measures between 5XFAD and TgSwDI animals (R^2 = 0.09, p<.05). However, not all Aβ species explained a significant proportion of the variance. Aβ42I (p = *n.s.*), Aβ40S (p = *n.s.*), and Aβ40I (p = *n.s.*) all did not contribute significantly to the difference in latency to find measures between animal groups. Aβ42S (p<.05) was the only Aβ species that accounted for a significant part of the variance in latency to find measures.

Immunohistochemistry and stereological measures.

In order to get a sampling of Aβ deposition in the brain as well as microvessels associated with Aβ42 plaques and microglial activation in the 5XFAD and TgSwDI animals, the animals with the highest, median, and lowest levels of total Aβ measures in the ELISA at 3 and 6 months of age were assessed. Cortex, subiculum, and thalamus were looked at (figure 6). Table 2 shows the results of all animals assessed on all measures arranged by age, brain region, and measure.

3 Months

Behavior.

In order to account for possible motor, anxiety, and activity level derived confounds that might affect the learning measures that were used in the Barnes maze, both 3 and 6 month old animals were assessed on the wire hang, rota-rod, light/dark box, 0-maze, and Digiscan apparatus. At 3 months of age, there were no significant differences in wire hang ($F[2,14] = .34$, $p = n.s.$) and Rota-rod ($F[2,14] = .64$, $p = n.s.$) measures, demonstrating that TgSwDI, 5XFAD, and WT animals all performed comparably on these tasks evaluating motor coordination, limb strength and endurance, and motor learning. In addition, there was no difference in the amount of time animals spent in the different quadrants of the light/dark box ($F[2,14] = 3.11$, $p = n.s.$) or O maze ($F[2,14] = 1.69$, $p = n.s.$), signifying that anxiety for light versus dark and open versus closed spaces was also not different between the TgSwDI, 5XFAD, and WT animals. Finally, there was no difference in the amount of rearings animals made in the Digiscan ($F[2,14] = 1.49$, $p = n.s.$) and no difference in horizontal activity measures ($F[2,14] = 1.83$, $p = n.s.$), further confirming findings regarding the lack of a difference between transgenic animal groups on limb strength, endurance, and activity level measures. However, a significant difference was found in the number of traversals made in the light/dark box ($F[2,14] = 4.99$, $p<.05$) as well as ambulation

motor activity in the Digiscan (F[2,14] = 4.05, p<.05). Fisher's post-hoc analysis determined that TgSwDI (M = 287, SD = 58.18) mice showed lower ambulation measures than either 5XFAD (M = 42, SD = 104.8, p<.05) or WT (M = 459.8, SD = 164.59, p<.05) mice. Meanwhile, there was not a significant difference between ambulation in the 5XFAD and WT animals (p = .79). Similarly, TgSwDI (M = 2.3, SD = 3.2) animals differed from 5XFAD (M =15.17, SD = 11.14, p<.05) and WT (M = 21.2, SD = 14.04, p<.05) animals in the number of traversals made in the light/dark box, but 5XFAD and WT animal comparisons showed no significant difference (p= *n.s.*). These comparisons suggest that there is a possible activity level difference that could confound Barnes maze learning measures. However, that the horizontal measure was not significantly different between the transgenic and WT groups suggest that contrasts in ambulation measures may have been artifactual.

In the Barnes maze spatial working memory task, it was found that there was a significant difference between the 5XFAD, TgSwDI, and WT mice in latency to find (F[2,14] = 8.03, p<.05) and latency to enter (F[2,14] = 7.07, p<.05) but not error measures (F(2,14) = .76, p = *n.s.*). A prior comparisons of the 5XFAD and TgSwDI animals showed that the 5XFAD transgenic had shorter latency to find (F [1,11] = 6.59, p<.05) and latency to enter (F[1,11] = 9.52, p<.05) measures. However, there were no differences between these groups in errors made (F[1,11] = .94, p = *n.s.*) In order to determine the rate of learning of the animals, a simple regression analysis was performed using the number of trials as the independent variable and the latency to find measure as the dependent variable. The latency to find measure was used instead of latency to enter or errors because it was found during testing that while animals consistently showed increased attention to the escape hole in the Barnes Maze, they often did not enter it right after discovery. In addition, they often explored multiple holes after initial contact with the

escape hole. The slope of the best-fit line for the simple regression was used as the "Barnes Maze Learning" measure. This was deemed to not be significant at the 3 month time point (F[2,14] = 1.59, p = *n.s.*).

ELISA.

As expected from earlier studies, there was a significant difference between TgSwDI and 5XFAD in most measures of ELISA for Aβ species. This included Aβ42 soluble (F[1,10] = 10.09, p<.05), Aβ42 insoluble (F[1,10] = 22.73, p<05), and Aβ40 soluble (F[1,10] = 22.74, p<.05). The measure for Aβ40 insoluble (F[1,10] = 3.67, p = *n.s.*) showed a trend towards significance but was not significantly different between TgSwDI and 5XFAD animals at the 3 month time point. In addition, aggregate measures of total Aβ42 (F[1,10] = 22.42, p<.05), Aβ40 (F[1,10] = 4.03, p,<05), and total Aβ (F[1,10] = 19.91, p,<05) showed that 5XFAD animals, true to their genotype, expressed a much larger load of all species of Aβ in their brains as compared to TgSwDI. Finally, the total Aβ42 measure was divided by total Aβ40 to determine the ratio of the two Aβ species. This was done because it was important to investigate the reported difference in Aβ42 to Aβ40 ratios in the TgSwDI vs. 5XFAD mice. As expected from previous findings, this different was highly significant (F[1,10] = 23.28, p,<05). These results demonstrate that at the 3 month time point, all measures of Aβ were significantly higher for the 5XFAD mouse versus the TgSwDI. However, Aβ42/Aβ40 ratios in these transgenic mice differ drastically so that 5XFAD animals produce a large quantity of Aβ42 and miniscule amounts of Aβ40 while TgSwDI mice exhibit the reverse pathology.

6 Months

Behavior.

Behavioral results at the 6-month time point closely resembled those at 3 months. There was still no significant differences seen on the wire hang (F[2,18] = .149, p = *n.s.*) or Rota-rod (F[2,18] = 2.26, p = *n.s.*) measures. In addition, no significant difference was seen in time spent in the different parts of the light/dark box (F[2,18] = 2.15, p = *n.s.*) or the O-maze (F[2,18] = 1.47, p = *n.s.*). Rearings made in the Digiscan (F[2,18] = 2.07, p = *n.s.*) was also not significantly different between the different groups. These data demonstrate that as mice aged to the 6 month time points, there were no significant changes in limb strength, coordination, endurance, or anxiety measures.

Interestingly, the number of transitions made in the light/dark box, which was a significant measure at 3 months, became non-significant at 6 months (F[2,18] = 1.54, p = *n.s.*) while the horizontal activity measures at 6 months (F[2,18] = 1.54, p = *n.s.*) remained comparable to findings in the younger age group.

At the 6 month time points, while the latency to find measure (F[2,18] = 5.58, p<.05) remained significant, the latency to enter (F[2,18] = .37, p = *n.s.*) and error measures (F[2,18] = 2.72, p = .09) became non-significant. Again, a prior comparisons between the 5XFAD and TgSwDI animals at this age showed that both groups were equally impaired on latency to find (F[1,11] = 2.89, p = *n.s.*), latency to enter (F[1,11] = 0.99, p = *n.s.*), and error measures (F[1,11] = 0.07, p = *n.s.*). Furthermore, the Barnes Maze Learning measure, which was non-significant at the 3 month time point, was still non-significant with this older age group (F[2,18] = 2.61, p = *n.s.*). These data suggest that all transgenic groups were significantly impaired on latency to find in the Barnes maze as compared to age-matched WTs in the 6 month age group.

ELISA.

At the 6 month time point, all measures of ELISA were significant, including Aβ42 soluble (F[1,12] = 6.12, p<.05), Aβ42 insoluble (F[1,12] = 8.72, p<.05), Aβ40 soluble (F[1,12] = 6.36, p<.05), and Aβ40 insoluble (F[1,12] = 5.84, p<.05). Aggregate measures of Aβ42 (F[1,12] = 7.47, p<.05), Aβ40 (F[1,12] = 5.33, p<.05), and total Aβ (F[1,12] = 7.53, p<.05) were also significant as well as the ratio of Aβ42/Aβ40 (F[1,12] = 4.55, p<.05). It should be noted that while the differences in Aβ levels remained significant between TgSwDI and 5XFAD animals, the overall levels of Aβ were much higher at the 6 month time point in both groups of animals versus at the 3 month time point (see figure 2).

Chapter 6

The amyloid cascade theory states that the build-up of Aβ in the brain leads to deleterious downstream effects such as neuroinflammation and cell death, which in turn cause the cognitive dysfunction seen in AD. The driving force behind AD research for the past decade and a half since its first introduction, this theory (Hardy & Higgins, 1992) has since undergone a lot of scrutiny and revision due to findings regarding many different aspects of Aβ, including the exact pathogenic form of the protein and where it is deposited. The goal of the present study was to investigate the specific association between parenchymal Aβ deposition, CAA, and cognitive decline seen in AD. In order to do so, two strains of transgenic animals, the 5XFAD and TgSwDI were employed as models of parenchymal Aβ deposition and CAA respectively. These transgenics were chosen due to previous findings documenting the unique parenchymal and CAA phenotypes expressed by the 5XFAD and TgSwDI respectively, as well as their robustly different levels of Aβ accumulation throughout development (Davis et al., 2004; Oakley et al., 2006; Xu et al., 2007). A secondary goal of the present study was to look at the contribution of the different species of Aβ as well as total levels of Aβ on cognitive dysfunction. Finally, a tertiary goal was to confirm previous findings regarding the mouse models used in the present study. It was expected that the 5XFAD and TgSwDI animals would express differential patterns of Aβ accumulation in the parenchyma as well as in the form of CAA and that total Aβ42 and Aβ40 species levels in these murine models would contrast greatly through development. Furthermore, these differences in the transgenic murine models were expected to be associated with performance on a spatial working memory task.

The present study found that while overall levels of Aβ42 and Aβ40 species were a predictor of cognitive dysfunction at 3 and 6-months of age in the 5XFAD and TgSwDI animals,

these measures did not tell the whole story. Instead, amyloid deposition in the parenchyma and as CAA was also found to be associated with the presence and onset of spatial working memory deficits. More specifically, these findings suggest that CAA and parenchymal amyloid deposition play differential roles in AD-like memory changes that are associated with the progression of the disease.

Behavioral Analysis and the Barnes Maze

The non-cognitive behavioral battery used in the present study including the wire hang, Rotarod, 0-maze, light-dark box, and Digiscan served two major purposes. The first was to test for differences in motor, anxiety, and overall activity levels in the 5XFAD and TgSwDI mouse models. The second was to address possible confounding factors that might have influenced measures looking at aspects of spatial working and reference memory in the Barnes maze. It has been previously argued that the Barnes maze apparatus relies primarily on the rodent's inherent fear of wide open and brightly lit spaces and preference for enclosed, dark areas as the main means of motivation (Pompl, Mullan, Bjugstad, & Arendash, 1998). In this sense, it is an appealing aversively motivated spatial learning/memory task in that it does not require any rigorous motor activity or appetitive reinforcer, both of which may exert undesirable counfounds on measures of learning (Harrison, Hosseini, & McDonald, 2008). In the present study, the 0-maze and light-dark box were used to assess possible anxiety confounds. Meanwhile, the wire hang, Rotarod, and Digiscan measures were used to assess possible motor and activity level confounds. It was found that age matched 5XFAD, TgSwDI, and WT animals in both age groups performed comparably on all non-cognitive behavioral tasks suggesting that Aβ pathology in the transgenic animals had a very selective effect on behavior.

The choice to use the present non-cognitive battery of behavioral tasks allowed us to confirm that differences observed in the Barnes maze measure between the 5XFAD and TgSwDI were not due to certain anxiety, activity level, and motor differences. However, it must be noted that because these tests were conducted before assessment in the Barnes maze, animals may have lost a measure of anxiety driven motivation that could have influenced results on the spatial working memory task. That is, all animals were previously handled before Barnes maze testing, which may have served to decrease the inherent anxiety that is a key motivating factor in the task (Barnes, 1979).

Confirming Previous Findings on the 5XFAD and TgSwDI

The TgSwDI and 5XFAD transgenic animals used in the present study served as mouse models of CAA and parenchymal Aβ deposition respectively. To date, there have only been two previous reports looking at spatial working and reference memory in the TgSwDI mouse (Fan et al., 2007; Xu et al., 2007) and only one report looking at non-spatial motor and anxiety performance as well as activity level (Xu et al., 2007). Meanwhile, although a number of studies have looked at different aspects of memory performance in the 5XFAD including contextual fear conditioning, object recognition, and Y-maze alternation (Joyashiki, Matsuya & Tohda, 2011; Kimura & Ohno 2009; Oakley et al., 2006; Ohno, 2009; Ohno et al., 2007), only one has employed a robust spatial working memory task in which the Morris Water maze was used (Urano & Todha, 2010) and only one has looked at non-spatial motor and anxiety performance as well as activity level (Jawhar et al., 2010). This illustrates that although these murine models are crucial to illustrating Aβ pathology and its effects on cognition, there is a relative paucity of studies characterizing these models behaviorally. Due to the observations that the 5XFAD mouse model exhibited a possible phenotypic deficit in motor functioning at 9 and 12 months of age

(Jawhar et al., 2010), the present study used the Barnes maze spatial working memory task which, when compared to the Morris Water maze, has spatial learning measures that are less likely to be influenced by possible motor and anxiety confounds, and when compared to the Y-maze, may be more sensitive to cognitive deficits (Arendash et al., 2001; Harrison et al., 2008).

Consistent with previous reports, the TgSwDI mouse did not exhibit motor, anxiety, or activity level deficits compared with age-matched WTs in either the 3 or 6 month age group. However, as previously mentioned, the TgSwDI showed a significant impairment compared to WTs in the ambulation measure in the Digiscan, which tracks movement parallel to the plane at both 3 and 6 month age groups though they were not impaired in the related, horizontal movement measure which detects all vertical and horizontal movement of the animal. These findings suggest that while TgSwDI may engage in less exploration than either the 5XFAD or WT animals, they were not impaired in overall activity level.

The Barnes maze task conducted in the present study validates previous findings of impaired performance of the TgSwDI at 3 months of age. However, here we demonstrate that even when animals were heterozygous for the human APP transgene, and produced significantly lower levels of overall Aβ40 and Aβ42 as compared to homozygous animals (Xu et al., 2007), they still experienced significant impairments in latency to find measures. In fact, in the 6-month age group, the heterozygous TgSwDI animals still produced significantly lower levels of Aβ40 and Aβ42 compared to homozygous animals at the 3-month time point in the Xu et al. (2007) study, but continued to show impaired latency to find performance compared with WTs in the Barnes maze. Latency to enter measures in the TgSwDI was similarly higher than age-matched controls at the 3-month age group. This suggests that TgSwDI animals were not only slower to find the escape box, but also slower to enter it. One possible explanation for this is

lowered anxiety or heightened activity levels in these transgenic animals. However, that the 0-maze and light/dark box measures were non-significant and ambulation activity was actually lower in the TgSwDI compared to age-matched WT at this age argue against this idea. Furthermore, error measures in the Barnes maze at 3 months were non-significant, revealing that both TgSwDI and WT animals explored the maze an equal amount. In 6 month old animals, the latency to enter difference seen at the earlier age is no longer significant. This finding, along with the significant difference in latency to find measures, shows that the TgSwDI animals are in fact, at 6 months of age, entering the escape hole more quickly than age-matched WT animals after discovering it. Again, though, that anxiety measures in both the 0-maze and light/dark box were non-significant argue against increased anxiety as the cause for this difference.

While motor, anxiety, and activity level changes have been investigated in the 5XFAD mouse, they have never been done so in animals at 3 and 6 months of age. The present results suggest that although intraneuronal Aβ42 accumulation starts at around the 3 month time point, there are no associated motor, anxiety or activity level changes that appeared as a result (Oakley et al., 2006). Furthermore, the 6-month age group also experienced no motor, anxiety, or activity level changes. This stands in contrast to previous reports demonstrating decreased anxiety of 5XFAD starting at 6 months when compared to age-matched WT animals (Jawhar et al., 2010). This inconsistency may be due to the gender differences between 5XFAD animals. Whereas Jawhar et al., (2010) included only female 5XFAD animals, the present study uses both males and females, though when ambulation measures were compared between genders, there was no significant difference found between the sexes (data not shown). Previous reports also note motor dysfunction in the wire hang and balance beam measures, but similar to the present

findings, these changes were only documented in older, 9 month old animals (Jahwar et al., 2010).

Previous reports investigating behavioral deficits of the 5XFAD mouse show that onset of cognitive disruption did not begin until after 5 months of age. In both contextual fear conditioning, Morris water maze, and Y-alternation tasks, the 5XFAD performed comparably to age matched WT animals before the 4-5 month time point and only began showing disruptions in remote memory retrieval and spatial working memory beyond 6 months (Kaczorowski et al., 2009; Kimura & Ohno, 2009; Ohno et al., 2007; Ohno, 2009; Urano & Tohda, 2010). Interestingly, the Barnes maze results in the present study confirm these findings. Animals at the younger 3 month time point showed no differences compared to age matched WT mice in latency to find measures and demonstrated a decreased latency to find compared to age matched TgSwDI. It was only in the later, 6 month age group that latency to find measures were significantly impaired compared to WTs. These findings suggest that not only are 5XFAD animals impaired in reconsolidation of contextual fear memory (Ohno, 2009) and alternation learning (Ohno et al., 2007), but also in aspects of spatial working and reference memory where contextual cues need to be encoded, consolidated, and retrieved.

In summary, the present findings confirm and supplement previous reports of normal motor, anxiety, and activity level functioning in the TgSwDI and 5XFAD animals. In addition, they show that TgSwDI animals heterozygous for the APP transgenes were nevertheless impaired in aspects of spatial working and reference memory. Finally, these results support previous work demonstrating that a number of different memory deficits surface only after the 5-6 month age point in the 5XFAD animals.

Parenchymal Aβ Deposition and AD-like Memory Changes

One of the most prominent pathological changes that occurs in and is associated with AD is the deposition of Aβ plaques in the parenchyma of the brain. These can be divided into two main categories, diffuse and focal deposits. Diffuse amyloid deposits are characterized mainly by low immunoreactivity, wide range of deposition, and a lack of association with dystrophic neurons and activated microglia and astrocytes. Meanwhile, the focal deposit category is further divided into non-neuritic or neuritic plaques. The main distinguishing factor between these two types is that while non-neuritic plaques have been shown to be comprised mainly of Aβ40, neuritic plaques are characterized by a dense, fibrillar amyloid core comprised mainly of the Aβ42 species surrounded by microglia, astroglia, and dystrophic neurites (Duyckaerts et al., 2009).

Here, the 5XFAD mouse is used as a prime model of fibrillar amyloid pathology in the parenchyma due to the rapid accumulation and deposition of Aβ42 as fibrillar amyloid plaques in the subiculum, hippocampus, cortex, and thalamus. In addition, the unique phenotype of these transgenics, which causes rapid deposition of amyloid plaques, allows for the chance to study the progression of cognitive dysfunction as it relates to Aβ accumulation in the brain through a series of developmental time points (Oakley et al., 2006). In contrast, the TgSwDI animals exhibit minimal amyloid plaque deposition in the parenchyma due to a phenotype which leads to predominantly mutant Aβ40 production and accumulation that is more prone to aggregate in the microvasculature (Davis et al., 2004). Comparing the progression of cognitive dysfunction in these two strains of transgenic animals at 3 and 6 months of age allowed for the unique opportunity to assess the contribution of fibrillary amyloid plaque deposition in the parenchyma to learning and memory deficits.

When comparing the 5XFAD and TgSwDI animals, one of the first and most important parameters to consider is the nature of their Aβ deposition. First, as can be seen from figure 4, the 5XFAD at both 3 and 6 months of age exhibit a pattern of dense staining of individually defined Aβ deposits in the subiculum. Meanwhile, the TgSwDI animals at 3 and 6 months of age show a much more continuous pattern of staining with Aβ where individually defined deposits are difficult to distinguish. Previous reports show that this pattern of staining is consistent with the presence of β–pleated sheet structure deposits of amyloid plaques in the 5XFAD animals (Oakley et al., 2006) and the presence of diffuse amyloid plaque deposition in the TgSwDI (Xu et al., 2007). Second, although area fraction analysis of total Aβ40 and Aβ42 and % microvessels associated with fibrillary amyloid plaques showed higher overall staining and percentages in the 5XFAD animals, the total Aβ40 and Aβ42 area fraction measure was reversed in the subiculum of 3 month old animals. Here, the TgSwDI animals that were chosen to represent the group showed overall higher levels of staining than their 5XFAD counterparts in this brain region. Furthermore, the percentage of microvessels associated with fibrillary plaques was higher overall in the TgSwDI group at both 3 and 6 months of age in the subiculum. These data demonstrate that compared to the 5XFAD, the TgSwDI animals deposit Aβ primarily and indeed almost exclusively in the subiculum at both 3 and 6 months of age. Furthermore, although the TgSwDI exhibits much lower levels of overall amyloid plaque deposition, consistent with previous reports, a much larger proportion of it is concentrated in the cerebral microvasculature of the subiculum (Davis et al., 2004).

The present findings in the 5XFAD suggest that there is a complex relationship between parenchymal amyloid plaque deposition and cognitive dysfunction. That the 5XFAD animals performed comparably to age-matched WTs at 3 months of age despite robust accumulation of

Aβ40 and Aβ42 in the fibrillary amyloid plaque form in the subiculum, cortex, and thalamus demonstrates that amyloid plaque deposition and the presence of Aβ in these brain areas do not necessarily predict cognitive dysfunction. The observation that only with increasing densities of Aβ and amyloid plaque deposition in all brain areas investigated at 6 months of age did latency measures in the Barnes maze see a decline in the 5XFAD, suggests that there may be a possible threshold of Aβ burden that needs to be reached before the pathology starts to influence cognitive function in an observable manner. Previous findings in another, widely used transgenic animal, the Tg2576, support this assertion. Numerous studies investigating the relationship between amyloid deposition and behavioral deficits in these animals paint an inconclusive picture. Some report a lack of association between amyloid plaque burden, increasing levels of Aβ, and behavioral deficits (Holcomb et al., 1999). Others show that while initial Aβ deposition produces no behavioral deficits, only a >10-fold increase in overall Aβ levels at a much later age leads to cognitive dysfunction (Hsiao et al., 1996). Still others suggest that a critical level of Aβ needs to accumulate in order to facilitate the formation of insoluble amyloid fibrils, and that these may result in behavioral disruption that may then still not be profound enough to be detected in all behavioral tasks (Westerman et al., 2002). All of these findings point to the importance of an accumulated volume of Aβ in the parenchyma that then must trigger some other downstream effects which leads to the emergence of cognitive dysfunction.

Taking a closer look at the individual animals chosen for Aβ density analysis as well as the percentage of microglia associated with amyloid plaques, it is apparent that while these two measures may not necessarily predict performance deficits, they may serve as a critical indicator. At the 3-month time point, the 5XFAD animal that had the highest Aβ area fraction and percentage of microvessels performed near the bottom half in Barnes maze learning measures.

Meanwhile the 5XFAD animal that had the lowest overall levels on both of these measures performed at the top of the group in the Barnes maze learning measure. Furthermore, this trend continued at the 6-month time point so that the 5XFAD animals that showed the highest and lowest measures on Aβ area fraction and percentage of microvessels respectively, demonstrated the flattest and steepest Barnes maze learning measures. Therefore, although the Aβ area fraction and percentage of microvessel measures do not strictly correlate with behavioral measures in the present study, this limited analysis suggests that they may be useful in indicating the presence, absence, or large-scale severity of memory changes in the 5XFAD.

In summary, the present results show that parenchymal deposition of Aβ in the fibrillar amyloid plaque form is not strongly correlated with the presence or severity of behavioral deficits. The onset of memory changes in the 5XFAD animals at 6 months of age suggest that a critical mass of Aβ must accumulate in the brain parenchyma before it begins to affect cognitive functioning. However, looking forward, it is apparent that in the TgSwDI animals, the idea of the importance of a critical level of Aβ build-up in the brain may not be as important as other factors of Aβ deposition in producing cognitive change. This possibility is discussed in the following section.

CAA and AD-like Memory Changes

Although the amyloid cascade theory has focused primarily on the parenchymal deposition of Aβ in the brain, the contributions of Aβ and amyloid plaque accumulation in the microvasculature is increasingly seen as a large contributing factor to cognitive and pathological symptoms of AD. One of the primary reasons for this is the role that the cerebral microvasculature has been described to play in the maintenance of a balance between Aβ production and elimination in and out of the brain. It is thought that Aβ clearance from the

extracellular space is facilitated by the cortical capillaries and arteries that feed into the periarterial space present between the sheath surrounding the arteries that provide the cortical blood supply, and the arachnoid sheath that surrounds the surface of the brain. Once Aβ enters this area, it is subsequently cleared along with other extracellular material through the interstitial fluid (for a more detailed discussion, see Nicoll et al., 2004). However, in CAA, instead of clearing from the perivascular space, Aβ aggregates along vessel walls, obstructing the elimination pathway, eventually leading to parenchymal deposition and other deleterious downstream effects. Aside from its hypothesized role in AD where CAA is often seen as a comorbid disorder, it has also been shown to cause stroke and dementia by itself, independent of other symptoms of AD (Kumar-Singh, 2008; Natte et al., 2001; Vinters, 1987; Yamada, 2002).

In the present study, we sought to investigate the effect of CAA on cognitive dysfunction by using the TgSwDI mouse model. The TgSwDI carries the Dutch and Iowa mutations on the APP gene which ultimately cause an overproduction of overall Aβ as well as a mutated form of Aβ40 that is prone to fibrillize and deposit in the cerebral microvasculature as opposed to the parenchyma (Davis et al., 2004; Herzig, Eisele, Staufenbiel, Jucker 2009; Tomidokoro et al., 2010). Whereas the TgSwDI animals had significantly lower levels of Aβ40 and Aβ42 in the forebrain at both the 3 and 6 month age than the 5XFAD, surprisingly, they exhibited memory deficits earlier than 5XFAD. Thus, a factor other than the overall forebrain levels of Aβ be a more important causal factor in initial cognitive decline in these animals, and perhaps also in AD patients.

When looking at the analyses of percentage of microvessels associated with amyloid plaques, it is clear that even though the TgSwDI had much lower levels of overall Aβ than the 5XFAD at both 3 and 6 months of age, they had comparable measures of % microvessels

associated with amyloid plaques, especially in the subiculum. Furthermore, in the 6 month animals that were investigated for percentage of microvessels, the TgSwDI had a higher percentage of amyloid plaque associated microvessels than age matched 5XFAD. How this elevation strictly correlates with performance in the Barnes maze learning measure is difficult to evaluate due to the observation that unlike the 5XFAD animals, TgSwDI individual rankings in the % microvessels associated with amyloid plaque deposition did not predict rankings in the Barnes maze learning measure. However, previous reports show that the presence of vascular amyloid plaque deposition is associated with a worse cognitive outcome compared to parenchymal amyloid plaque deposition alone and that this is particularly prominent in the earliest stages of AD related dementia (Esiri et al., 1999; Zekry et al., 2002). In fact, this viewpoint predicts the present findings well. While the 5XFAD animals produced a large amount of Aβ at the 3 month time point, the stereological findings in our sample suggest that only a small proportion of it was deposited in the microvasculature. This time point correlates with the starting point of pathology in these animals (Oakley et al., 2006; Ohno 2009) and they performed comparable to age-matched WT animals at this age. Comparatively, the TgSwDI animals, which performed poorly on the Barnes maze task at 3 months of age, produced very low overall levels of Aβ, but the present stereological sample suggests that a large proportion was deposited as amyloid plaques in the microvasculature.

Presently, the mechanisms behind the effect of CAA on cognitive dysfunction in the earliest stages of AD are unclear. However, there have been a number of studies investigating the pathological effects of Aβ deposition in the microvasculature and a couple of different factors have emerged as potentially disrupting cognitive function. First, evidence suggests that Aβ accumulation in the vessel walls not only causes degeneration of the vascular system and its

components, but also ischemia (Wisniewski et al., 2000) and eventually, microhemorrhaging (Herzig, Van Nostrand, Jucker, 2006; Nicoll et al., 2004). Consequently, microhemmoraging is a well documented contributor to disruption of learning and memory deficits (Wilcock & Colton, 2009) and is also a feature seen in the TgSwDI mouse around the age that cognitive decline is first reported (Davis et al., 2004). Second, similar to the neuronal inflammation associated with amyloid plaques in the parenchyma seen in AD, perivascular inflammation has also been seen in CAA (Eng et al., 2004). This feature is again, seen in the TgSwDI animals starting at the 3 month time point, correlating well with the onset of behavioral changes. Third, and finally, while the cerebral microvasculature is seen as a transport system for Aβ, it is often cited as being complementary to transport of Aβ out of the brain directly through the blood brain barrier (BBB; Nicoll et al., 2004). Therefore, the presence of CAA can be interpreted as a sign of degeneration of the BBB (Kumar-Singh, 2008).

In summary, while the TgSwDI animals did not exhibit higher overall levels of Aβ compared with the 5XFAD, they did display more profound memory deficits at 3 months of age as well as comparable percentages of microvessels associated with amyloid plaques in both age groups. This suggests that vascular deposition of Aβ has a more pronounced effect on cognitive performance compared to parenchymal deposition at an earlier developmental stage in these animals. It is possible that the mechanism behind the influence of CAA on cognitive decline characteristic of AD may be through its association with ischemia or microhemmoraging, perivascular inflammation, or as a precursor to breakdown of the BBB.

The Interaction between Parenchymal Aβ Deposition and CAA

While it may be tempting to suggest that either deposition of Aβ in the parenchyma or the microvasculature is the main cause of cognitive deficits seen in AD, the more logical conclusion

and one that is increasingly supported by the literature suggests that CAA and parenchymal Aβ deposition have synergistic effects. Two key lines of research point to this idea. The first is high percentage of comorbidity of CAA in AD patients and the increasing diagnosis of mixed dementia as a combination of vascular plus AD pathologies. The second is the possible mediating function that the ApoE ε4 allele serves in both increasing the severity and likelihood of CAA and AD. Both of these considerations will be discussed in terms of how they support the synergistic effect of CAA and parenchymal deposition of Aβ in AD pathology.

Comorbidity of CAA and AD and Mixed Dementia (MD).

One of the most striking observations among the elderly population suffering from AD is the presence of CAA as a comorbid disorder. The presence of CAA in AD has been cited as anywhere from 94%-100% of patients and it has been shown to decrease the age of onset and increase the severity of symptoms during the early stages of dementia (Jellinger & Attems, 2005; Jellinger & Attems, 2007; Nicoll et al., 2004). Meanwhile, complications associated with CAA and vascular dementias appear to correlate well with cognitive dysfunction. For example, in a study of normal healthy elderly individuals, the presence of infarcts was associated with a much higher risk for dementia related disease later in life (Vermeer et al., 2003). In addition, predictors of vascular disease such as artheroslerosis and ventricular dysfunction increase the likelihood of AD (Kalaria, 2000). Furthermore, vascular changes such as decreased clearance of Aβ, decreased surface area of the capillary basement membrane, and decreased cerebral blood flow appear to become more severe with progression AD pathology (Jellinger & Attems, 2007). These interactions between the symptoms of CAA and AD and the cognitive decline that appears as a result have suggested the idea that these diagnoses may in fact, be at the opposite sides of a

spectrum of Aβ related disorders with some significant overlap in both physiological and cognitive symptoms.

Although the classification of pathologies for MD is not entirely agreed upon (Del Ser, Hachinski, Merskey, & Munoz, 2005) and even the mere presence of the disorder as an entity separate from AD and CAA is up for debate, the acknowledgement of MD as a combination of symptoms of the two other disorders is well documented (Gold et al., 2007; Jellinger & Attems, 2007). What is especially interesting to note however, are studies showing that the incidence of CAA decreases with age while the incidence of AD and MD appear to increase (Jellinger & Attems, 2010). These findings fit well with data suggesting an impact of CAA on earlier stages of AD that appear to diminish in effect at later ages (Esiri et al., 1999; Zekry et al., 2002).

In summary, vascular pathologies characteristic of CAA are often seen as predisposing factors to AD and the presence of CAA in a high percentage of AD cases is well documented (Jellinger & Attems, 2005; Jellinger & Attems, 2007; Nicoll et al., 2004). This, coupled with the increasing diagnosis of MD as a combination of AD as well as vascular dementias related to CAA suggest that these two diseases are intimately related and may in fact, be at opposite ends of a spectrum of disorders that are caused by Aβ deposition in the parenchyma and vasculature of the cortex.

Apoe ε4.

Although the ApoE gene is not present in the 5XFAD or TgSwDI, it is important to consider the effect of the gene and its different alleles due to the role that it plays in balancing the deposition of Aβ in the parenchyma and microvasculature. The ApoE gene and its different alleles, especially the ε4 allele (apoe4) has long been known to be one of the only genetic contributors to the onset and severity of the spontaneous form of AD (Strittmatter et al., 1993). The number of

apoe4 alleles that an individual carries can not only affect age of onset, but also severity of AD as well as overall speed of progression of symptoms (Corder et al., 1993; Roses, 1996). The Apoe protein is produced in high quantities in the liver with lower levels present in the brain where it is generated mainly by astrocytes but also in small amounts by neurons (Kim, Basak, Holtzman, 2009). It functions mainly as a ligand and in forms of cholesterol transport along with other lipoproteins (for an in-depth review, see Kim et al., 2009).

In the context of the present study, apoe4 is interesting in the role that it plays in affecting the balance of pathologies seen in both CAA and AD. These roles range from affecting the balance between Aβ40 and Aβ42 and the pathological properties of each (Fryer et al., 2005), to causing changes in the cerebral microvasculature (Donahue & Johanson, 2008) to distributing Aβ preferentially to the vasculature or parenchyma (Fryer et al., 2005; Xu et al., 2008). Each of these factors suggests the apoe4 allele decreases the age of onset and increases the severity of AD due to its function in shifting Aβ production and deposition towards a pathological pattern more representative of CAA with AD than AD alone. These changes in turn, may lead to the earlier appearance of cognitive disruption as seen in the TgSwDI mouse versus the 5XFAD.

Apoe4 has been shown to increase the ratio of Aβ40 to Aβ42 in AD through the production of an increased amount of the former species and furthermore, an increase in its fibrillogenic properties (Fryer et al., 2005; Mann et al., 1997). This increase is correlated with a decreased age of onset of AD and CAA and resulting cognitive disruption which presents earlier in age (Corder et al., 1993; Roses, 1996). These changes parallel the phenotype of the TgSwDI animals, which, although produce increased amounts of Aβ40 versus Aβ42 due to a different mechanism (Dutch and Iowa APP gene mutations), likewise exhibit highly fibrillogenic

Aβ40 (Davis et al., 2004) and a behavioral disruption in spatial working memory that precedes that seen in the 5XFAD who do not exhibit the same ratio of Aβ species.

Another effect of the apoe4 allele that has been reported is its detrimental influence on the cerebral microvasculature, more specifically, in decreasing the cerebral capillary membrane surface area (Donahue & Johanson, 2008). It is possible that this decrease in turn increases the likelihood of CAA due to impaired transport of Aβ through a compromised cerebral microvasculature, coinciding then, with an earlier age of onset and an increased severity of cognitive deficits seen in AD. In fact, previous reports in the TgSwDI have reported the presence of microhemmoraging (Davis et al., 2004), a sign, not only of a compromised vascular system due to CAA, but also a harbinger for cognitive dysfunction (Wilcock & Colton, 2009).

Probably the most salient finding of the function of apoe4 in suggesting a connection between CAA and AD and the role of the former in increasing the symptoms and decreasing the age of onset of cognitive dysfunction in the later, is how it changes the deposition of Aβ. Many studies have shown that apoe4 preferentially shifts amyloid plaque deposition from the parenchyma into the vasculature (Chalmers, Wilcock, Love, 2003; Fryer et al., 2005; Schmechel et al., 1993). This is again, temporally correlated with an earlier age of onset of the spontaneous form of AD in patients that carry the apoe4 allele and is also in line with reports of the presence of CAA in AD causing earlier and more severe development of symptoms (Esiri et al., 1999; Zekry et al., 2002).

In summary, the finding that the apoe4 allele influences the age of onset and severity of AD and CAA suggests that it plays a critical role in both of these disorders (Corder et al., 1993; Roses, 1996; Strittmatter et al., 1993; Thal et al., 2002). However, the observation that apoe4 shifts the ratio of Aβ40:42, redistributes amyloid plaque deposition, and degrades the cerebral

microvasculature suggests that it may act through CAA to influence the degree of severity of AD. Furthermore, that these same CAA factors that are affected by apoe4 in humans, are present in the TgSwDI mouse which, compared to the 5XFAD in the present study experience cognitive dysfunction at an earlier age, again points to the critical role that CAA plays in AD.

Aβ40 and Aβ42 Levels and AD-like Memory Changes

Up until this point, the present study has focused on the effect of Aβ deposition in the parenchyma vs. the vasculature and the effect of this spatial deposition on cognitive dysfunction. However, it is important to note that this is not the only important contrast between the 5XFAD and TgSwDI animals. As illustrated by figure 2, another large difference between these transgenic strains is the amount of total Aβ being produced and the ratio of Aβ42 to Aβ40 that exists. Consistent with previous reports, the 5XFAD animals produced about 30 to 50 times more total Aβ than TgSwDI and Aβ42/40 in a ratio of roughly 8:1 at 3 months of age and about 6:1 at 6 months of age while the TgSwDI animals exhibited the opposite effect, producing Aβ42/40 at about 1:3 at 3 months of age and about 1:6 at 6 months of age (Davis et al., 2004; Oakley et al., 2006). While previous research has largely implicated Aβ42 as the main pathological species responsible for fibrillary amyloid plaque accumulation in AD (Iwatsubo et al., 1994; Younkin, 1998), it is apparent that in the present study, this does not necessarily translate into cognitive dysfunction. In fact, it is the TgSwDI, with a higher ratio of Aβ40 to Aβ42 that shows cognitive impairment as measured by the Barnes maze in the younger age group. These observations suggest two main possibilities. The first is the idea that Aβ40 itself plays a large role in the early development of cognitive dysfunction. The second is the idea that elevated levels of Aβ40 leads to deposition of amyloid preferentially in the microvasculature as opposed to the parenchyma and it is, again, the spatial location of amyloid plaque that is leading to cognitive dysfunction.

Although Aβ42 has long been implicated as the more fibrillary, pathogenic species present in the brains of AD patients, recent studies are demonstrating that the mutant form of Aβ40 processed as a result of the Dutch and Iowa APP mutations is far from benign. Studies have noted the cytotoxic effects of mutant Aβ40 on smooth muscle cells in the cerebral microvasculature through the triggering of the apoptotic cell death cycle (Davis, Cribbs, Cotman, & Van Nostrand, 1999; Van Nostrand et al., 2002). Yet in spontaneous AD, Aβ40 has been shown to have a more neuroprotective effect. Yan and Wang (2007) demonstrated that Aβ40 both protects neurons from the neurotoxic effects of Aβ42 and prevents its aggregation into the more toxic oligomeric and fibrillar confirmations (Yan & Wang, 2008). Therefore, a high ratio of wild-type Aβ40 to Aβ42 species may actually serve a preventative role, even though this is not reflected in the 5XFAD animals, whose increasing Aβ40 to Aβ42 ratio from 3 to 6 months did not have an effect on cognitive performance as assessed in the Barnes maze.

While evidence argues against the role of wild type Aβ40 as a direct contributor to the cognitive dysfunction seen in AD, it has been shown to be a large player in CAA pathology, particularly in the context of the Dutch and Iowa FAD mutations. Previous reports looking at the effect of the Dutch and Iowa mutations shows that the altered form of Aβ40 that is generated in these cases show both a higher tendency towards fibrillization and a propensity for deposition in the cerebral microvasculature and thereby, inhibiting Aβ clearance from the brain (Davis et al., 2006; Herzig et al., 2009; Tomodikoro et al., 2010). However, as noted before, this is not restricted to mutant forms of Aβ40. In fact, the ratio of wild-type Aβ42/Aβ40 can also determine amyloid deposition. Whereas an elevated ratio of Aβ42/Aβ40 increases the likelihood of parenchyma deposition, a lowered ratio of Aβ42/Aβ40 instead shifts deposition to the microvasculature (Herzig et al, 2006). Furthermore, while Aβ42 appears to form the core of

amyloid deposits in the microvasculature and is essential for initial aggregation, it is the Aβ40 species that comprises the larger portion of the amyloid plaques in this area (McGowan et al., 2005). These findings support observations made in the present study. While 5XFAD animals had overall higher levels of Aβ42 and Aβ40 in the ELISA measures, it is possible that the elevated Aβ42/Aβ40 ratio partially contributed in shifting amyloid deposition to the parenchyma. Meanwhile, although TgSwDI had comparatively lower levels of both Aβ42 and Aβ40 species, the lower ratio of Aβ42/Aβ40 may have lead to aggregation in the vasculature.

In summary, the role of Aβ40 and by association, the ratio of Aβ40 to Aβ42, on AD and CAA largely appears to depend on the form it takes. While wild-type Aβ40 has been shown to serve a primarily benign or beneficial role in AD (Yan & Wang, 2008), the mutated Dutch and Iowa forms of the protein are implicated as a pathological species in CAA (Davis et al., 1999; Davis et al., 2006; Herzig et al., 2009; Tomodikoro et al., 2010; Van Nostrand et al., 2002). These views are consistent with the findings in the present study. While wild-type Aβ40 levels did not appear to have a large effect on the cognitive performance of the 5XFAD, elevated levels of Dutch/Iowa mutant Aβ40 may have played a significant role in the behavioral deficits seen in the young and older age groups in the TgSwDI mice.

Chapter 7

Clinical Implications

The results of the current study suggest that the spatial deposition of amyloid in the brain in either the parenchyma or the microvasculature has an earlier impact on cognitive function than overall accumulating levels of total Aβ40 and Aβ42. More specifically, amyloid plaque deposition in a form resembling CAA appears to lead to spatial memory deficits at an age point in transgenic mice that resembles the earliest stages of AD. In light of the recent advancement in immunotherapy treatments as a possible option for AD patients, these findings serve as a cautionary observation that abolishing the brain of parenchyma amyloid deposits may not address one of the key sources of cognitive dysfunction.

Recent immunotherapy trials have implemented one of two main procedures. The first is passive immunity, injecting Aβ antibodies directly into a subject and the second is active immunity, injecting Aβ into a subject to allow for the natural formation of antibodies by the subjects own immune system. Regardless of which type of immunotherapy is used, the majority of studies have reported a beneficial effect of Aβ removal on cognitive functioning (Wilcock & Colton, 2009). However, these findings underscore two main problems with this procedure. The first is that immunotherapy often causes encephalitis and neuroinflammation in a small proportion of patients (Gandy, 2005). The second is that while parenchymal amyloid plaque deposits appear to be removed by immunotherapy, multiple reports have described an increased occurrence of CAA in both transgenic animals and humans (Nicoll et al., 2003; Wilcock et al., 2004; Wilcock et al., 2006; Wilcock et al., 2007). Presumably, this increase is due to the failure of a clearance of Aβ by antibodies through the cerebrovascular system and into the periphery (WIlcock & Colton, 2009). As might be predicted from the results of the present study, long term

assessment of cognitive functioning after immunization often revealed an inconsistent recovery of cognitive deficits which may be due to the persisting presence of CAA (Arendash et al., 2001; Holmes et al., 2008).

The present results coupled with existing literature on immunotherapy studies suggest that while Aβ immunotherapy may target one contributor to the cognitive symptoms seen in AD, namely amyloid deposition in the parenchyma, it may be exacerbating another. Immunotherapy procedures must not only abolish parenchymal amyloid deposition, but also prevent CAA at the same time. Therefore, treatments that target the source of Aβ toxicity may ultimately prove to be the most fruitful avenues of research. Two of these include anti-aggregation drugs that prevent Aβ from forming amyloid oligomers and as a result, fibrillary plaques, and α–secretase promoters that increase the role of the enzyme in processing APP in order to bias production of other forms of Aβ against Aβ42 (Gandy, 2005).

Future Directions

The present study looked at the effect of parenchymal deposition of Aβ versus CAA on the appearance and progression of cognitive dysfunction representative of AD using the 5XFAD and TgSwDI mouse models respectively. The Barnes maze apparatus was used to assess aspects of spatial working memory and ELISA measures revealed levels of Aβ species in 3 and 6 month old animals. In addition, a sampling of animals in the 3 and 6 month age groups were observed on microvessels associated with thioflavinS positive plaques, total amyloid, and activated microglia measures. It was found that while high levels of Aβ predicted cognitive changes in the 5XFAD in the 6 month age group, it did not do so in the younger 3 month age group. Meanwhile although Aβ levels were low overall in the TgSwDI compared to the 5XFAD at both 3 and 6 months of age, these animals exhibited cognitive change in both age groups. When looking at an

immunohistochemical sampling of the TgSwDI, it was found that these animals had an overall larger percentage of Aβ associated with the microvasculature compared to 5XFAD, especially in the subiculum.

Although the present study looked at microvessels associated with fibrillary amyloid plaques, it did not investigate the microhemorraging and other vascular changes that often occurs as a result (Davis et al., 2004). This phenomenon has been reported in the TgSwDI though not in the 5XFAD which do not exhibit elevated levels of Aβ deposition in microvessels at any age (Davis et al., 2004; Oakley et al., 2006). Microhemmoraging and alteration of the cerebral vascular system has been described to be a major contributor of cognitive changes in the past (Kalaria, 1996; Zekry et al., 2002) although these changes have also been described to lack an effect on studies of spatial working memory (Wilcock et al., 2004). It would be interesting to see then, whether microhemorraging is a factor that differentiates the 5XFAD and TgSwDI and how this difference contributes to observed cognitive changes.

Due to the observations made in the current study, it would be interesting to evaluate the effect of Aβ immunotherapies that addresses CAA rather than parenchymal deposition of Aβ on cognitive changes seen in the TgSwDI. Previous reports investigating the effect of anti-Aβ antibodies on the TgSwDI have reported that although immunotherapy was successful in clearing diffuse amyloid plaques in the parenchyma, they did not remedy vascular amyloid plaques and recovery of cognitive functioning was not assessed afterwards (Vasilevko et al., 2007). Clinical trials reveal that for the most part, there is a balance between parenchymal deposition of Aβ and CAA. While immunotherapy decreases amyloid plaque accumulation in the parenchyma, most often vascular amyloid deposition increases as a result (Vasilevko et al., 2010). However, other studies have suggested that CAA may decrease with time and that

repeated long term administration of anti-Aβ immunotherapy starting at an early age can facilitate the removal of amyloid deposition in the microvasculature (Boche et al., 2008; Prada et al., 2007; Thakker et al., 2009; Vasilevko et al., 2010). It may be important then, to assess long-term anti-Aβ immunotherapy in the TgSwDI to see if symptoms of CAA in these animals are reduced with time. Furthermore, potential cognitive recovery should be evaluated to see if there is a correlation between the removal of Aβ from the vasculature and improvement of cognitive functioning. The potential clinical implications of these findings are the possible implementation of a gradual passive anti-Aβ immunotherapy that targets CAA symptoms during the earliest stages of AD, thereby preventing degradation of the Aβ clearance system in the brain and downstream Aβ accumulation in the parenchyma.

Conclusion

The findings of the present study demonstrate that while the ACT proposes a main cause for AD that is clear and testable, the viewpoint is still very much a work in progress. Though Aβ is a large contributor to AD-like cognitive change, small details pertaining to different aspects of Aβ such as the species of Aβ and where it is deposited, can have a huge impact on whether it is predictive of cognitive change or not. Here, we demonstrate that absolute levels of Aβ are only predictive of cognitive impairment to a certain extent and that furthermore, while Aβ manifesting as CAA is a key player in early stages of AD-like cognitive change, Aβ deposited in the parenchyma appears to be more predictive during later stages of the disease.

References

Alzheimer A. (1907). Ueber eine eigenartige Erkrankung der Hirnrinde [On a peculiar disease of the cerebral cortex]. *Zeitschrift fuer Psychiatrie,* 64: 146

Alzheimer's Association. *Stages of Alzheimer's*, Retrieved June 9, 2011 from http://www.alz.org/alzheimers_disease_stages_of_alzheimers.asp

Arendash GW., Gordon MN., Diamond DM., Austin LA., Hatcher JM., Jantzen P., DiCarlo G., Wilcock D., Morgan D. (2001). Behavioral assessment of Alzheimer's transgenic mice following long-term Aβ vaccination: task specificity and correlations between Aβ deposition and spatial memory. *DNA and Cell Biology,* 20: 737-744

Barnes CA. (1979) Memory deficits associated with senescence: a neurophysiological and behavioral study in the rat. *Journal of Comparative and Physiological Psychology* 93:74-104

Bayer TA., Wirths O., Majtenyi K., Hartmann T., Multhaup G., Beyreuther K., Czech C. (2001). Key factors in Alzheimer's disease: b-amyloid precursor protein processing, metabolism and intraneuronal transport. *Brain Pathology,* 11: 1-11

Bitan G., Fradinger FA., Spring SM., Teplow DB. (2005). Neurotoxic protein oligomers – what you see is not always what you get. *Amyloid,* 12: 88-95

Boche D., Zotova E., Weller RO., Love S., Neal JW., Pickering RM., Wilkinson D., Holmes C., Nicoll JA. (2008). Consequences of Abeta immunization on the vasculature of human Alzheimer's disease brain. *Brain,* 131: 3299-3310

Castellani RJ., Smith MA., Perry G., Friedland RP. (2004). Cerebral amyloid angiopathy: major Contributor or decorative response to Alzheimer's disease pathogenesis. *Neurobiology of Aging,* 25: 599-602

Chalmers K., Wilcock GK., Love S. (2003). Apoe epsilon 4 influences the pathological phenotype of Alzheimer's disease by favoring cerebrovascular over parenchymal accumulation of Abeta protein. *Neuropathology and Applied Neurobiology,* 29: 231-238

Corder EH., Saunders AM., Strittmatter WJ., Schmechel DE., Gaskell PC., Small GW., Roses AD., Haines JL., Pericack-Vance MA. (1993). Gene dose of apolipoprotein E type 4 allele and the risk of Alzheimer's disease in late onset families. *Science,* 261: 921- 923

Cummings BJ. & Cotman CW. (1995). Image analysis of beta-amyloid loid in Alzheimer's disease and relation to dementia severity. *Lancet,* 346: 1524-1528

Davis J., Cribbs DH., Cotman CW., Van Nostrand WE. (1999). Pathogenic amyloid beta-protein induces apoptosis in cultured human cerebrovascular smooth muscle cells. *Amyloid,* 6: 157-164

Davis J. & Van Nostrand WE. (1996). Enhanced pathologenic properties of Dutch-type mutant amyloid-beta protein. *Proceedings of the National Academy of Sciences of the USA,* 93: 2996-3000

Davis J., Xu F., Deane R., Romanov G., Previti ML., Zeigler K., Zlokovic BV., Van Nostrand WE. (2004). Early-onset and robust cerebral miscrovascular accumulation of amyloid β–protein in transgenic mice expressing low levels of a vasculotropic Dutch/Iowa mutant form of amyloid. *Journal of Biological Chemistry,* 279: 20296-20306

Davis J., Xu F., Miao K., Previti ML., Romanov G., Ziegler K., Van Nostrand WE. (2006). Deficient cerebral clearance of vasculotropic mutant Dutch/Iowa double Aβ in AβPP transgenic mice. *Neurobiology of Aging,* 27: 946-954

Del Ser T., Hachinski V., Merskey H., Munoz DG. (2005). Alzheimer's disease with and without

cerebral infarcts. *Journal of the Neurological Sciences,* 231: 3-11

Donahue JE. & Johanson CE. (2008). Apolipoprotein E, amyloid-β and blood-brain barrier permeability in Alzheimer disease. *Journal of Neuropathology and Experimental Neurology,* 67: 261-270

Duff K. (1997). Alzheimer transgenic mouse models come of age. *TINS,* 20: 279-280

Duyckaerts C., Delatour B., Potier M. (2009). Classification and basic pathology of Alzheimer disease. *Acta Neuropathologica,* 118:5-36

Duyckaerts C., Potier MC., Delatour B. (2008). Alzheimer disease models and human neuropathology: similarities and differences. *Acta Neuropathologia,* 115: 5-38

Elder GA., Gama Sosa MA., Gasperi RD. (2010). Transgenic mouse models of Alzheimer's disease. *Mount Sinai Journal of Medicine,* 77: 69-81

Eng JA., Frosch MP., Choi K., Rebeck GW., Greenberg SM. (2004). Clinical manifestations of cerebral amyloid angiopathy-related inflammation. *Annals of Neurolog,* 55: 250-256

Esiri MM., Nagy Z., Smith MZ., Barnetson L., Smith AD. (1999). Cerebrovascular disease and threshold for dementia in the early stages of Alzheimer's disease. *Lancet,* 364: 919-920

Esler & Wolfe (2001). A portrait of Alzheimer secretases-new features and familiar faces. *Science,* 239:1449-1454

Fan R., Xu F., Previti ML., Davis J., Grande AM., Robinson JK., Van Nostrand WE. (2007). Minocycline reduces microglial activation and improves behavioral deficits in a transgenic model of cerebral vascular amyloid. *Journal of Neuroscience,* 27: 3057-3063

Fryer JD., Simmons K., Parsadanian M., Bales KR., Paul SM., Sullivan PM., Holzman DM. (2005). Human apolipoprotein E4 alters the amyloid-beta 40:42 ratio and promotes the

formation of cerebral amyloid angiopathy in an amyloid precursor protein transgenic model. *Journal of Neuroscience,* 25: 2803-2810

Gandy S. (2005). The role of cerebral amyloid β accumulation in common forms of Alzheimer disease. *Journal of Clinical Investigation,* 115: 1121-1129

Goate A., Chartier-Harlin MC., Mullan M., Brown J., Crawford F., Fidani L., Giuffra L., Haynes A., Irving N., James L. (1991). Segregation of a missense mutation in the amyloid precursor protein gene with familial Alzheimer's disease. *Nature,* 349: 704-706

Gold G., Giannakopoulos P., Herrmann FR., Bouras C., Kovari E. (2007). Identification of Alzheimer and vascular lesion thresholds for mixed dementia. *Brain,* 130: 2830-2836

Guenette SY. & Tanzi RE. (1999). Progress toward valid transgenic mouse models for Alzheimer's disease. *Neurobiology of Aging,* 20: 201-211

Haglund M., Kalaria R., Slade JY., Englund E. (2006). Differential deposition of amyloid beta peptides in cerebral amyloid angiopathy associated with Alzheimer's disease and vascular dementia. *Acta Neuropathologica,* 111: 430-435

Hardy JA. & Higgins GA. (1992). Alzheimer's disease: the amyloid cascade hypothesis. *Science,* 256: 184-185

Harper JD., Wong SS., Lieber CM., Langsbury PT. (1997). Observation of Abeta amyloid protofibrils by atomic force microscopy. *Chemical Biology,* 4: 119-125

Harper JD., Wong SS., Lieber CM., Langsbury PT. (1999). Assembly of Abeta amyloid protofibrils: An in vitro model for a possible early event in Alzheimer's disease. *Biochemistry,* 38: 8972-8980

Harrison FE., Hosseini AH., McDonald MP. (2009). Endogenous anxiety and stress responses in

water maze and Barnes maze spatial memory tasks. *Behavioral Brain Research*; 198: 247-251

Herzig MC., Eisele YS., Staufenbiel M., Jucker M. (2009). ESSQ-mutant Aβ peptide (AβDutch) increases vascular but reduces parenchymal Aβ deposition. *American Journal of Pathology,* 174: 722-726

Herzig MC., Van Nostrand WE., Jucker M. (2006). Mechanism of cerebral beta-amyloid angiopathy: murine and cellular models. *Brain Pathology,* 16: 40-54

Holcomb LA., Gordon MN., Jantzen P., Hsiao K., Duff K., Morgan D. (1999). Behavioral changes in transgenic mice expressing both amyloid precursor protein and presinilin-1 mutations: lack of association with amyloid deposits. *Behavioral Genetics* 29: 177-185

Holmes C., Boche D., Wilkinson D., Yadegarfar G., Hopkins V., Bayer A., Jones RW., Bullock R., Love S., Neal JW., Zotova E., Nicoll JA. (2008). Long-term effects of Abeta42 immunization in Alzheimer's disease: follow up of a randomized, placebo-controlled phase 1 trial. *Lancet,* 372: 216-223

Hsiao K. & Ashe KH. (2001). Learning and memory in transgenic mice modeling Alzheimer's disease. *Learning and Memory,* 8: 301-308

Hsiao K., Chapman P., Nilsen S., Eckman C., Harigaya Y., Younkin S., Yang F., Cole G. (1996). Correlative memory deficits, Aβ elevation, and amyloid plaques in transgenic mice. *Science,* 274: 99-102

Iwatsubo T., Odaka A., Suzuki N., Mizusawa H., Nukina N., Ihara Y. (1994). Visualization of A beta 42(43) and A beta 40 in senile plaques with end-specific A beta monoclonals: evidence that an initially deposited species is A beta 42(43). *Neuron,* 13: 45-53

Jawhar S., Trawicka A., Jennecjens C., Bayer TA., Wirths O. (2010). Motor deficits, neuron

loss, and reduced anxiety coinciding with axonal degeneration and intraneuronal Aβ aggregation in the 5XFAD mouse model of Alzheimer's disease. *Neurobiology of Aging,* (in press)

Jellinger KA. & Attems J. (2005). Prevalence and pathogenic role of cerebrovascular lesions in Alzheimer's disease. *Journal of the Neurological Sciences,* 229-230: 37-41

Jellinger KA. & Attems J. (2007). Neuropathological evaluation of mixed dementia. *Journal of Neurological Sciences,* 27: 80-87

Jellinger KA. & Attems J. (2010). Is there pure vascular dementia in old age? *Journal of the Neurological Sciences,* 299: 150-154

Joyashiki E., Matsuya Y. & Tohda C. (2011). Sominone improves memory impairments and increases axonal density in Alzheimer's disease model mice, 5XFAD. *International Journal of Neuroscience,* 121: 181-190

Kaczorowski CC., Samestsky E., Shah S., Vassar R., Disterhoft JF. (2009). Mechanisms underlying basal and learning-related intrinsic excitability in a mouse model of Alzheimer's disease. *Neurobiology of Aging,* (in press)

Kalaria RN. (1996). Cerebral vessels in ageing and Alzheimer's disease. *Pharmacology & Therapeutics,* 72: 193-214

Kalaria RN. (2000). The role of cerebral ischemia in Alzheimer's disease. *Neurobiology of Aging,* 21: 321-330

Kawai M., Lalaria RN., Cras P., Siedlak SL., Velasco ME., Shelton ER., Chan HW., Greenberg BD., Perry G. (1993). Degeneration of vascular muscle cells in cerebral amyloid angiopathy of Alzheimer disease. *Brain Research,* 623: 142-146

Kim J., Basak JM., Holtzman DM. (2009). The role of apolipoprotein E in Alzheimer's disease.

Neuron, 63: 287-303

Kimura R., Davi L., Ohno M. (2010). Partial reduction of BACE1 improves synaptic plasticity, recent and remote memories in Alzheimer's disease transgenic mice. *Journal of Neurochemistry,* 113: 248-261

Kimura R. & Ohno M. (2009). Impairments in remote memory stabilization precede hippocampal synaptic and cognitive failures in 5XFAD Alzheimer mouse model. *Neurobiology of Disease,* 33: 229-235

Klein WL. (2002). Aβ toxicity in Alzheimer's disease: globular oligomers (ADDLs) as new vaccine and drug targets. *Neurochemistry International,* 41: 345-352

Kumar-Singh S. (2008). Cerebral amyloid angiopathy: pathogenetic mechanisms and link to dense amyloid plaques. *Genes, Brain and Behavior,* 7(Supp. 1): 67-82

Lemere CA. & Masliah E. (2010). Can Alzheimer disease be prevented by amyloid beta immunotherapy? *Nature Reviews. Neurology,* 6:108-119

Lesne S., Koh MT., Kotilinek L., Kayed R., Glabe CG., Yang A., Gallagher M., Ashe KH. (2006). A specific amyloid-beta protein assembly in the brain impairs memory. *Nature,* 440:352-357

Levy E., Carman MD., Fernandex-Madrid IJ., Power MD., Lieberburg I., van Duinen SG., Bots GTAM., Luyendijk W., Frangione B. (1990). Mutations of the Alzheimer's disease amyloid gene in hereditary cerebral hemorrhage, Dutch type. *Science,* 248: 1124-1126

Levy-Lahad E., Wasco W., Poorkaj P., Romano DM., Oshima J., Pettingell WH., Yu CE., Jondro PD., Schmidt SD., Wang K. (1995). Candidate gene for the chromosome 1 familial Alzheimer's disease locus. *Science,* 269: 973-977

Lewczuk P., Esselmann H., Otto M., Maler JM., Henkel AW., Henkel MK., Eikenberg O., Antz

C., Krause WR., Reulbach U., Kornhuber J., Wiltfang J. (2004). Neurochemical diagnosis of Alzheimer's dementia by CSF abeta 42, abeta 42/40 ratio, and total tau. *Neurobiology of Aging,* 25: 273-281

Lue LF., Kuo YM., Roher AE., Brachova L., Shen Y., Sue L., Beach T., Kurth JH., Rydel RE., Rogers J. (1999). Soluble amyloid beta peptide concentration as a predictor of synaptic chance in Alzheimer's disease. *The American Journal of Pathology,* 155: 853-962

Maness LM., Banks WA., Podlisny MB., Selkoe DJ., Kastin AJ. (1994). Passage of human amyloid beta-protein 1-40 across the murine blood-brain barrier. *Life Science,* 55: 1643-1650

Mann DM., Iwatsubo T., Pickering-Brown SM., Owen F., Saido TC., Perry RH. (1997). Preferential deposition of amyloid beta protein (Abeta) in the form Abeta40 in Alzheimer's disease is associated with a gene dosage effect of the apolipoprotein E E4 allele. *Neuroscience Letters,* 221: 81-84

McGowan E., Pickford F., Kim J., Onstead L., Eriksen J., Yu C., Skipper L., Murphy MP., Beard J., Das P., Jansen K., Delucia M., Lin WL., Dolios G., Wang R., Eckman CB., Dickson DW., Hutton M., Hardy J., Golde T. (2005). Abeta42 is essential for parenchymal and vascular amyloid deposition in mice. *Neuron,* 47(2): 191-199

McLean CA., Cherny RA., Fraser FW., Fuller SJ., Smith MJ., Beyreuther K., Bush AI., Masters CL. (1999). Soluble pool of Abeta amyloid as a determinant of severity of neurodegeneration in Alzheimer's disease. *Annals of Neurology,* 46: 860-866

Miravalle L., Tokuda T., Chiarle R., Giaccone G., Bugiani O., Tagliavini F., Frangione B., Ghiso J. (2000). Substitution at codon 22 of Alzheimer's abeta peptide induce diverse conformational changes and apoptotic effects in human cerebral

endothelial cells. *Journal of Biological Chemistry,* 275: 27110-27116

Morgan D., Diamond DM., Gotschall PE., Ugen KE., Dickey C., Hardy J., Duff K., Jantzen P., DiCarlo G., Wilcock D., Connor K., Hatcher J., Hope C., Gordon M., Arendash GW. (2000). A beta peptide vaccination prevents memory loss in an animal model of Alzheimer's disease. *Nature,* 408: 982-985.

Natte R., de Boer WI., Maat-Schieman ML., Baelda HJ., Vinters HV., Roos RA., van Duinen SG. (2001). Dementia in hereditary cerebral hemorrhage with amyloidosis-Dutch type is associated with cerebral amyloid angiopathy but is independent of plaques and neurofibrillary tangles. *Annals of Neurology,* 50: 765-772

Nicoll JA., Wilkinson D., Holmes C., Steart P., Markham H., Weller RO. (2003). Neuropathology of human Alzheimer disease after immunization with amyloid-beta peptide: a case report. *Nature Medicine,* 9: 448-452

Nicoll JA., Yamada M., Frackowiak J., Mazur-Kolecka B., Weller RO. (2004). Cerebral amyloid angiopathy plays a direct role in the pathogenesis of Alzheimer's disease Pro-CAA statement. *Neurobiology of Aging,* 25: 589-597

Nordberg A. (2004). PET imaging of amyloid in Alzheimer's disease. *Lancet Neurology,* 3: 519-527

Oakley H., Cole SL., Logan S., Maus E., Shao P., Craft J., Guillozet-Bongaarts A., Ohno M, Disterhoft J., Van Eldik L., Berry R., Vassar R. (2006). Intraneuronal β–amyloid aggregates, neurodegeneration, and neuron loss in transgenic mice with five familial Alzheimer's disease mutations: potential factors in amyloid plaque formation. *Journal of Neuroscience,* 26: 10129-10140

Oddo S., Caccamo A., Smith IF., Green KN., LaFerla FM. (2006). A dynamic relationship

between intracellular and extracellular pools of Aβ. *American Journal of Pathology,* 168: 184-194

Ohno M., Cole SL., Yasvoina M., Zhao J., Citron M., Berry R., Disterhoft JF., Vassar R. (2007). BACE1 gene deletion prevents neuron loss and memory deficits in 5XFAD APP/PS1 transgenic mice. *Neurobiology of Disease,* 26: 134-145

Ohno M. (2009). Failures to reconsolidate memory in a mouse model of Alzheimer's disease. *Neurobiology of Learning and Memory,* epub before print.

Pearson RC., Esiri MM., Hiorns RW., WIlcock GK., Powell TP. (1985). Anatomical correlates of the distribution of the pathological changes in neocortex in Alzheimer's disease. *Proclamation of the National Academy of Science,* 82: 4531-4534

Pfeifer M., Boncristiano S., Bondolfi L., Stadler A., Deller T., Staufenbiel M., Mathews PM., Jucker M. (2002). Cerebral hemorrhage after passive anti-Abeta immunotherapy. *Science,* 298: 1379

Pfeifer LA., White LR., Ross GW., Petrovitch H., Launer LJ. (2002). Cerebral amyloid angiopathy and cognitive function: the HAAS autopsy study. *Neurology,* 58: 1629-1634

Pimplikar SW. (2009). Reassessing the amyloid cascade hypothesis of Alzheimer's disease. *International Journal of Biochemistry and Cell Biology,* 41: 1261-1268

Pompl PN., Mullan MJ., Bjugstad K., Arendash GW. (1999). Adaptation of the circular platform spatial memory task for mice: use in detecting cognitive impairment in the APPsw transgenic mouse model of Alzheimer's disease. *Journal of Neuroscience Methods* 87:87-95

Prada CM., Garcia-Alloza M., Betensky RA., Zhang-Nunes SX., Greenberg SM., Bacskai BJ., Frosch MP. (2007). Antibody-mediated clearance of amyloid-beta peptide from cerebral amyloid angiopathy revealed by quantitative in vivo imaging. *Journal of Neuroscience,* 27: 1973-1980

Rensink AAM., de Waal RMW., Kremer B., Verbeek MM. (2003). Pathogenesis of cerebral amyloid angiopathy. *Brain Research Reviews,* 43: 207-223

Rogers J. & Morrison JH. (1985). Quantitative morphology and regional and laminar distributions of senile plaques in Alzheimer's disease. *Journal of Neuroscience,* 5: 2801-2808

Roses AD. (1996). Apolipoprotein E alleles as risk factors in Alzheimer's disease. *Annual Review of Medicine,* 47:387-400

Sair HI., Doraiswamy PM., Petrella JR. (2004). In vivo amyloid imaging in Alzheimer's disease. *Neuroradiology,* 46: 93-104

Schmechel DE., Saunders AM., Strittmatter WJ., Crain BJ., Hulette CM., Joo SH., Pericack-Vance MA., Goldgaber D., Roses AD. (1993). Increased amyloid beta-peptide deposition in cerebral cortex as a consequence of apolipoprotein E genotype in late-onset Alzheimer disease. *Proclamation of the National Academy of Science,* 90: 9649-9653

Selkoe DJ. (1994). Alzheimer's disease: a central role for amyloid. *Journal of Neuropathology and Experimental Neurology,* 53: 438-447

Shankar GM., Li S., Mehta TH., Garcia-Munoz A., Shepardson NE., Smith I., Brett FM., Farrell MA., Rowan MJ., Lemere CA., Regan CM., Walsh DM., Sabitini BL., Selkoe DJ. (2008). Amyloid-beta protein dimers isolated directly from Alzheimer's brains impair synaptic plasticity and memory. *Nature Medicine,* 14: 837-842

Shen J. & Kelleher III RJ. (2007). The presinilin hypothesis of Alzheimer's disease: evidence for a loss-of-function pathogenic mechanism. *PNAS,* 104: 403-409

Sherrington R., Rogaev EI., Liang Y., Rogaeva EA., Levesque G., Ikeda M., Chi H., Lin C., Li G., Holman K. (1995). Cloning of a gene bearing missense mutations in early-onset familial Alzheimer's disease. *Nature,* 375: 754-760

Skovronsky DM., Doms RW., Lee VM. (1998). Detection of a novel intraneuronal pool of insoluble amyloid beta protein that accumulate with time in culture. *The Journal of Cell Biology,* 141: 1031-1039

Smith EE. & Greenberg SM. (2009). β-Amyloid, blood vessels, and brain function. *Stroke,* 40: 2601-2606

Stopa EG., Butala P., Salloway S., Johanson CE., Gonzalez L., Tavares R., Hovanesian V., Hulette CM., Vitek MP., Cohen RA. (2008). Cerebral cortical arteriolar angiopathy, vascular beta-amyloid, smooth muscle actin, Braak stage, and ApoE genotype. *Stroke,* 39: 814-821

Strittmatter WJ., Saunders AM., Schmechel D., Pericak-Vance M., Enghild J., Salvesen GS. (1993). Apolipoprotein E: high-avidity binding to beta-amyloid and increased frequency of type 4 allele in late-onset Alzheimer disease. *Proclamation of the National Academy of Science,* 90:1977-1981

Teplow DB., Lazo ND., Bitan G., Bernstein S., Wyttenbach T., Bowers MT., Baumketner A., Shea JE., Urbanc B., Cruz L., Borreguero J., Stanley HE. (2006). Elucidating amyloid beta-protein folding and assembly: a multidisciplinary approach. *Accounts of Chemical Research,* 39: 635-645

Terry RD., Masliah E., Salmon DP., Butters N., DeTeresa R., Hill R., Hansen LA., Katzman R. (1991). Physical basis of cognitive alterations in Alzheimer's disease: synapse loss is the major correlate of cognitive impairment. *Annals of Neurology,* 4: 572-5804

Thakker DR., Weatherspoon MR., Harrison J., Keene TE., Lane DS., Kaemmerer WF., Stewart GR., Shafer LL. (2009). Intracerebroventricular amyloid-beta antibodies reduce cerebral amyloid angiopathy and associated micro-hemmorrhage in aged Tg2576mice. *Proclamation of the National Academy of Science,* 106:4501-4506

Thal DR., Capetillo-Zarate E., Larionov S., Staufenbiel M., Zurbruegg S., Beckmann N. (2009). Capillary cerebral amyloid angiopathy is associated with vessel occlusion and cerebral blood flow disturbances. *Neurobiology of Aging,* 30: 1936-1948

Thal DR., Ghebremedhin E., Rub U., Yamaguchi H., Del Tredici K., Braak H. (2002). Two types of sporadic cerebral amyloid angiopathy. *Journal of Neuropathology and Experimental Neurology,* 61: 282-293

Thal DR., Griffin WST., Braak H. (2008). Parenchymal and vascular Aβ–deposition and its effects on the degeneration of neurons and cognition in Alzheimer's disease. *Journal of Cellular and Molecular Medicine,* 12: 1848-1862

Tomidokoro Y., Rostagno A., Neubert TA., Lu Y., Rebeck WG., Frangione B., Greenberg SM., Ghiso J. (2010). Iowa variant of familial Alzheimer's disease. *American Journal of Pathology,* 176: 1841-1854

Urano T. & Todha C. (2010). Icariin improves memory impairment in Alzheimer's disease mouse model (5XFAD) and attenuates amyloid β–induced neurite atropy. *Phytotherapy Research,* 24: 1658-1663

Van Broekhoven C., Haan J., Bakker E., Hardy JA., Van Hul W., Wehnert A., Vegter Van der

Vlis M., Roos RA. (1990). Amyloid beta precursor protein gene and hereditary cerebral hemorrhage with amyloidosis (Dutch). *Science,* 248: 1120-1122

Van Nostrand WE., Melchor JP., Cho HS., Greenberg SM., Rebeck GW. (2001). Pathogenic effects of D23N Iowa mutant amyloid-beta protein. *Journal of Biological Chemistry,* 276: 32860-32866

Van Nostrand WE., Melchor JP., Romanov G., Zeigler K., Davis J. (2002). Pathogenic effects of cerebral amyloid angiopathy mutations in the amyloid-beta protein precursor. *Annals of the New York Academy of Science,* 977: 258-265

Vasilevko V., Passos GF., Quiring D., Head E., Kim RC., Fisher M., Cribbs DH. (2010). Aging and cerebrovascular dysfunction: contribution of hypertension, cerebral amyloid angiopathy, and immunotherapy. *Annals of the New York Academy of Science,* 1207: 58-70

Vasilevko V., Xu F., Previti ML., Van Nostrand WE., Cribbs DH. (2007). Experimental investigation of anibody-mediated clearance mechanisms of amyloid-β in CNS of Tg-SwDI transgenic mice. *Neurobiology of Disease,* 27: 13376-13383

Vermeer SE., Prins ND., de Heijer T., Hofman A., Koudstaal PK., Breteler MM. (2003). Silent brain infarcts and the risk of dementia and cognitive decline. *New England Journal of Medicine,* 348: 1215-1222

Villemagne VL., Fodero-Tavoletti MT., Pike KE., Cappai R., Masters CL., Rowe CC. (2008). The ART of loss: Abeta imaging in the evaluation of Alzheimer's disease and other dementias. *Molecular Neurobiology,* 38: 1-15

Vinters HV. (1987). Cerebral amyloid angiopathy. A critical review. *Stroke,* 18: 311-324

Vinters HV., Wang ZZ., Secor DL. (1996). Brain parenchymal and microvascular amyloid in

Alzheimer's disease. *Brain Pathology*, 6: 179-195

Walsh DM., Klyubin I., Fadeeza JV., Cullen WK., Anwyl R., Wolfe MS., Rowan MJ., Selkoe DJ. (2002). Naturally secreted oligomers of amyloid β protein potently inhibit hippocampal long-term potentiation *in vivo*. *Nature,* 416: 535-539

Walsh DM., Lomakin A., Benedek GB., Maggio JE., Condron MM., Teplow DB. (1997). Amyloid β-protein fibrillogenesis: detection of a protofibrillar intermediate. *Journal of Biological Chemistry,* 272: 22364-22374

Walsh DM. & Selkoe DJ. (2007). Aβ oligomers – a decade of discovery. *Journal of Neurochemistry,* 101:1172-1184

Westerman MA., Cooper-Blacketer D., Mariash A., Kotilinek L., Kawarabayashi T., Younkin L., Carlson GA., Younkin SG., Ashe KA. (2002). The relationship between Aβ and memory in the Tg2576 mouse model of Alzheimer's disease. *Journal of Neuroscience,* 22: 1858-1867

Wilcock DM., Alamed J., Gottschall PE., Grimm J., Rosenthal A., Pons J., Ronan V., Symmonds K., Gordon MN., Morgan D. (2006). Deglycosylated anti-amyloid-beta antibodies eliminate cognitive deficits and reduce parenchymal amyloid with minimal vascular consequences in aged amyloid precursor protein transgenic mice. *Journal of Neuroscience,* 26: 5340-5346

Wilcock DM. & Colton CA. (2009). Immunotherapy, vascular pathology, and microhemorrhages in transgenic mice. *CNS Neurological Disorder Drug Targets,*8: 50-64

Wilcock DM., Jantzen PT., Li Q., Morgan D., Gordon MN. (2007). Amyloid-beta vaccination,

but not nitro-nonsteroidal ati-inflammatory drug treatment, increases vascular amyloid and microhemorrhage while both reduce parenchymal amyloid. *Neuroscience,* 144(3): 950-960

Wilcock DM., Rojiani A., Rosenthal A., Subbarao S., Freeman MJ., Gordon MN., Morgan D. (2004). Passive immunotherapy against Abeta in aged APP-transgenic mice reverses cognitive deficits and depletes parenchymal amyloid deposits in spite of increased vascular amyloid and microhemorrhage. *Journal of Neuroinflammation,* 1:

Wilson CA., Doms RW., Lee VM. (1999). Intracellular APP processing and Abeta production in Alzheimer's disease. *Journal of Neuropathology and Experimental Neurology,* 58: 787-794

Wiltfang J., Esselmann H., Bibl M., Smirnov A., Otto M., Paul S., Schmidt B., Klafki HW., Maler M., Dyrks T., Bienert M., Beyermann M., Rüther E., Kornhuber J. (2002). Highly conserved and disease specific patterns of carboxyterminally truncated abeta peptides 1-37/38/39 in addition to 1-40/42 in Alzheimer's disease and patients with chronic neuroinflammation. *Journal of Neurochemistry,* 81: 481-496

Wirths O., Multhaup G., Czech C., Blanchard V., Moussaoui S., Tremp G., Pradier L., Beyreuther K., Bayer TA. (2001). Intraneuronal Abeta accumulation precedes plaque formation in β–amyloid precursor protein and presinilin-1 double-transgenic mice. *Neuroscience Letters,* 306: 116-120

Wisniewski HM., Wegiel J., Vorbrodt AW., Mazur-Kolecka B., Frackowiak J. (2000). Role of perivascular cells and myocytes in vascular amyloidosis. *Annals of the New York Academy of Sciences,* 903: 6-18

Xu F., Grande AM., Robinson JK., Previti ML., Vasek M., Davis J., Van Nostrand WE.

(2007). Early-onset subicular microvascular amyloid and neuroinflammation correlate with behavioral deficits in vasculotropic mutant amyloid β-protein precursor transgenic mice. *Neuroscience,* 146: 98-107

Xu F., Vitek MP., Colton CA., Previti ML., Gharkholonarehe N., Davis J., Van Nostrand WE. (2008). Human apolipoprotein E redistributes fibrillar amyloid deposition in Tg-SwDI mice. *Journal of Neuroscience,* 28: 5312-5320

Yamada M. (2002). Risk factors for cerebral amyloid angiopathy in the elderly. *Annals of the New York Academy of Science,* 977: 37-44

Yan C. & Wang Y. (2007). Abeta40 protects non-toxic Abeta42 monomer from aggregation. *Journal of Molecular Biology*, 369: 909-916

Yan C. & Wang Y. (2008). Protective mechanisms against Aβ42 aggregation. *Current Alzheimer's Research,* 5: 548-554

Younkin SG. (1998). The role of Aβ42 in Alzheimer's disease. *Journal of Physiology,* 92: 289-292

Zekry D., Duyckaerts C., Moulias R., Belmin J., Geoffre C., Herrmann F., Hauw J. (2002). Degenerative and vascular lesions of the brain have synergistic effects in dementia of the elderly. *Acta Neuropathologica,* 103: 481-487

Appendix A

Figure 1

Diagram showing different considerations of the Amyloid Cascade Theory. The first level illustrates the different conformations of Aβ implicated in AD. The second level illustrates the different areas that amyloid β has been shown to deposit and have a deleterious impact.

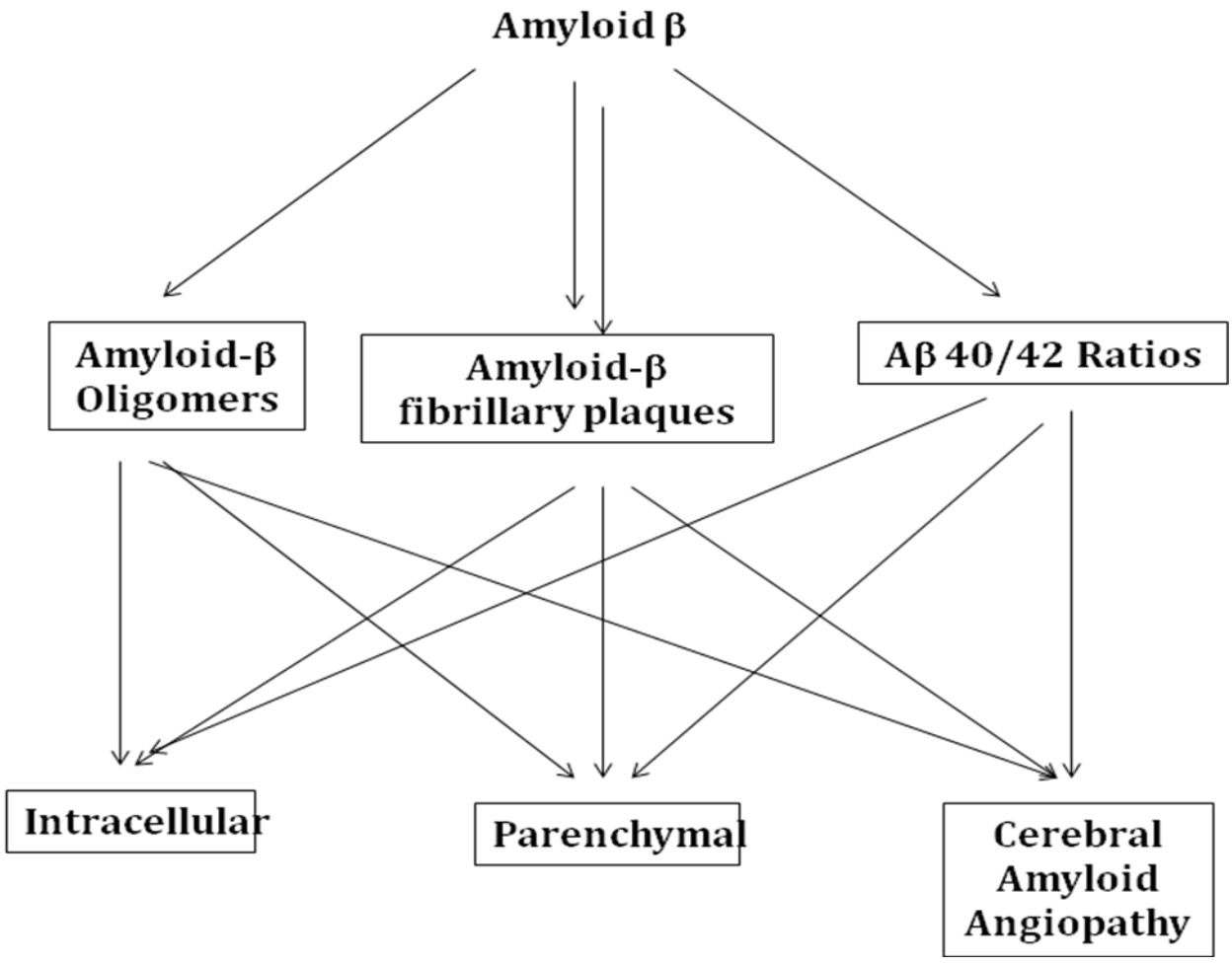

Figure 2

Graph showing the levels of each Aβ species in TgSwDI and 5XFAD mice at the a) 3 month and b) 6 month time points. Aβ load is measured in pg/mg. 5XFAD animals show higher levels of all species of Aβ in both the 3 and 6 month age groups.

a)

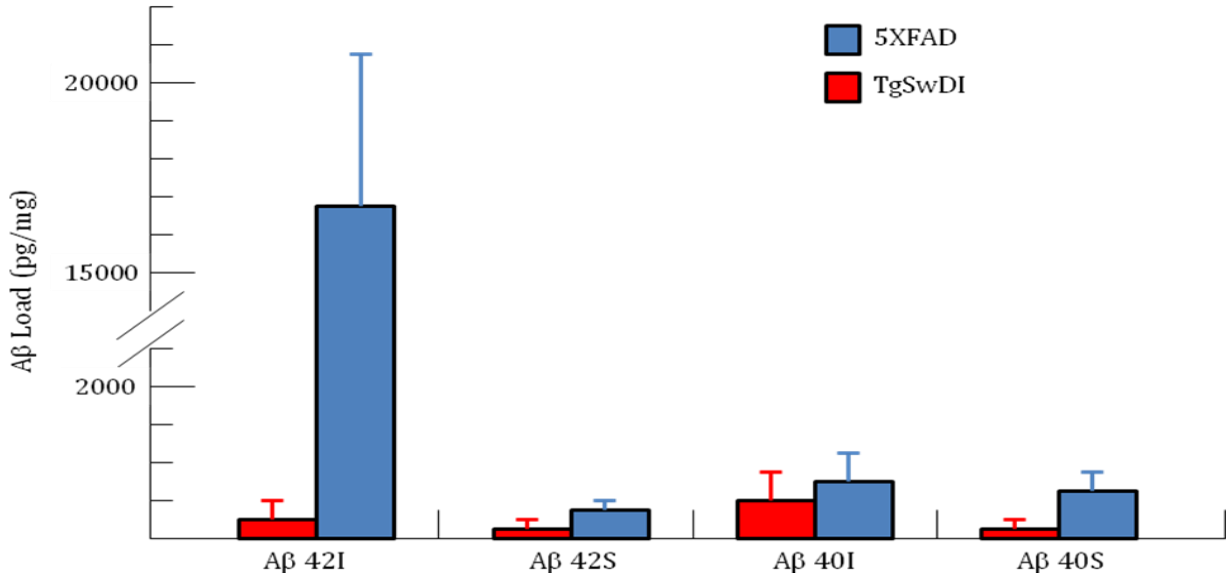

b)

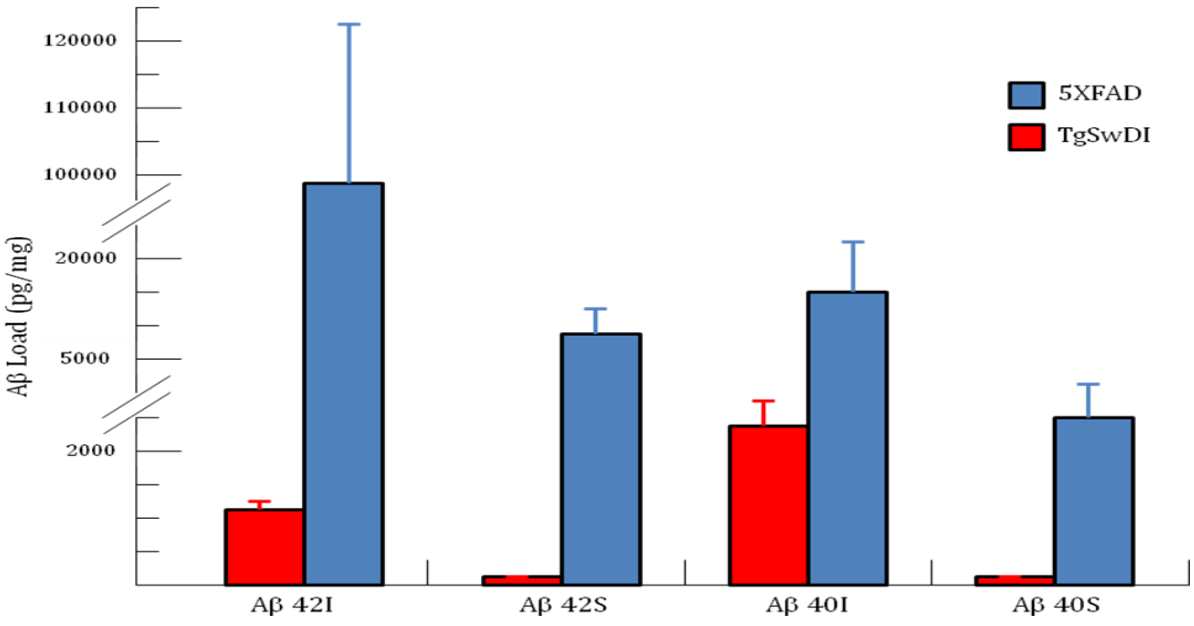

Figure 3

Graph showing 3 and 6 month age group performance on a & b) wire hang, c & d) Rotarod, e & f) 0-maze, g & h) Light/Dark box i & j) Digiscan rearing measures in the 5XFAD, TgSwDI, and WT animals. 3-month old wild type (Wild-Type 3), 6-month old wild type (Wild-Type 6), 3-month old TgSwDI (TgSwDI 3), 6-month old TgSwDI (TgSwDI 6), 3-month old 5XFAD (5XFAD 3), 6-month old 5XFAD (5XFAD 6). 5XFAD and TgSwDI animals performed comparably on all tasks compared to age-matched wild-type controls in both 3 and 6 month age groups. Error bars represent SEM.

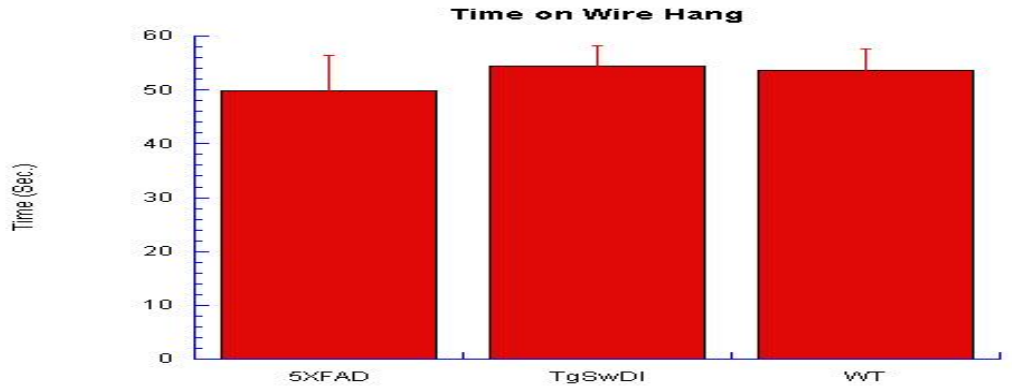

a)

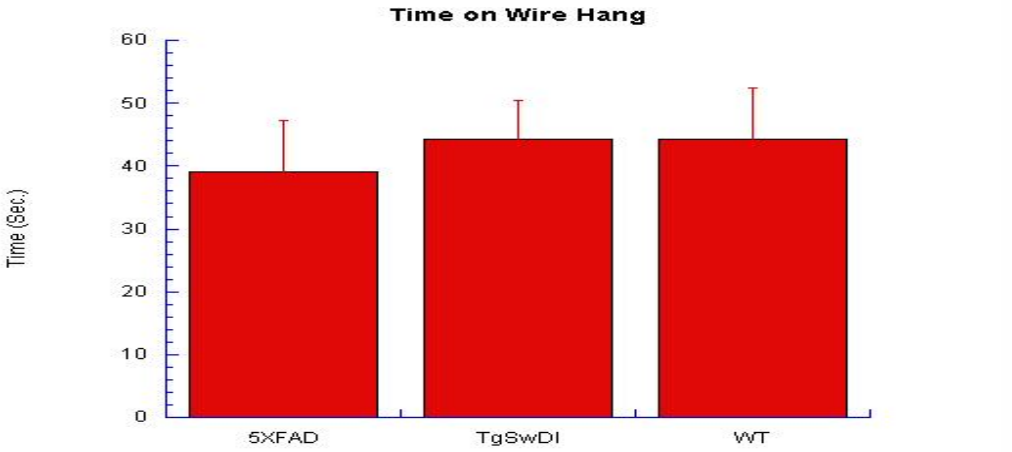

b)

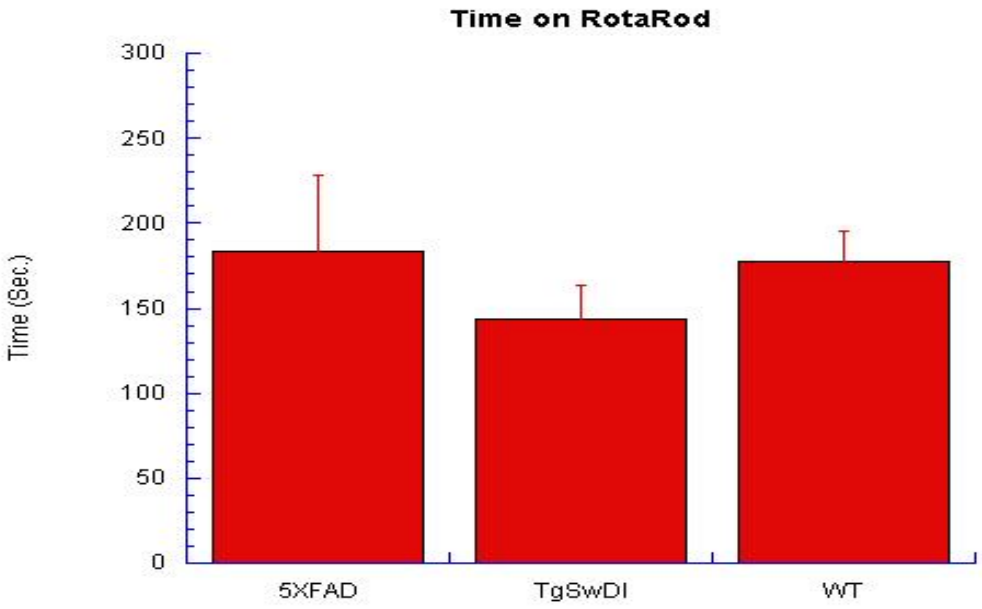
Time on RotaRod
Time (Sec.)
300
250
200
150
100
50
0
5XFAD
TgSwDI
WT

c)

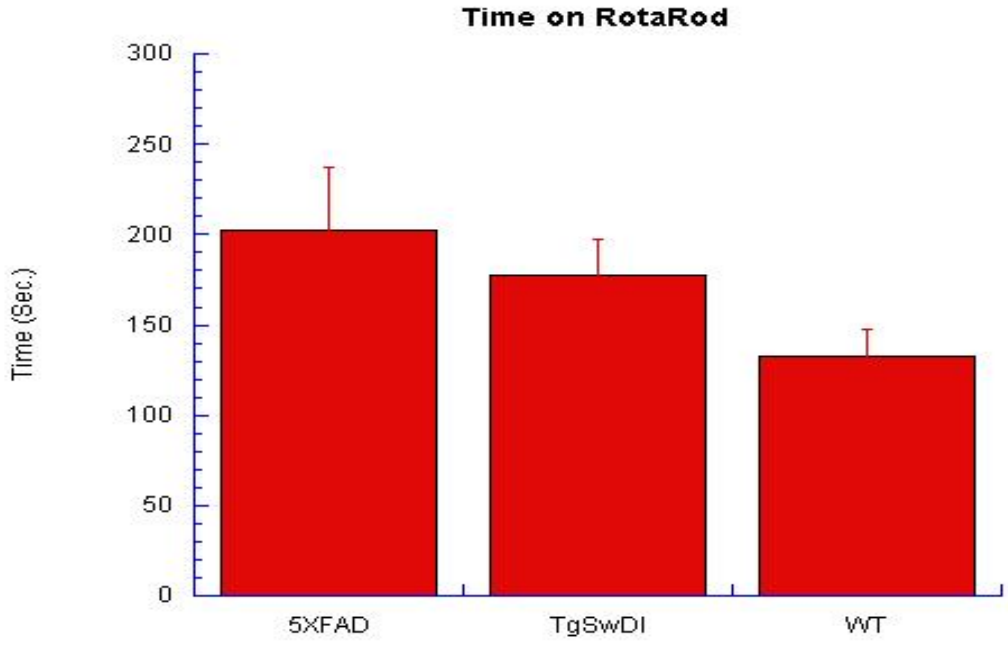
Time on RotaRod
Time (Sec.)
300
250
200
150
100
50
0
5XFAD
TgSwDI
WT

d)

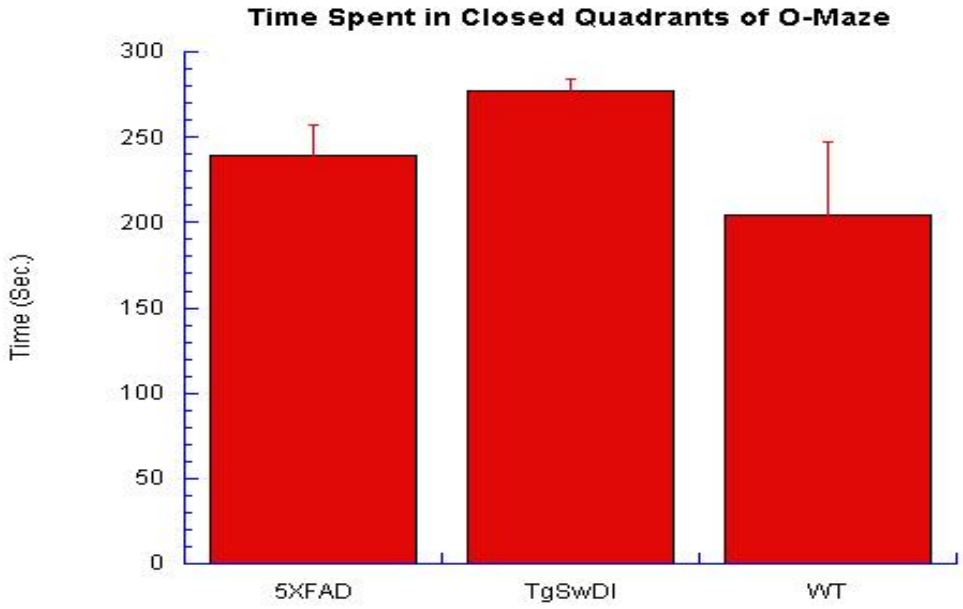
Time Spent in Closed Quadrants of O-Maze
Time (Sec.)
300
250
200
150
100
50
0
5XFAD
TgSwDI
WT

e)

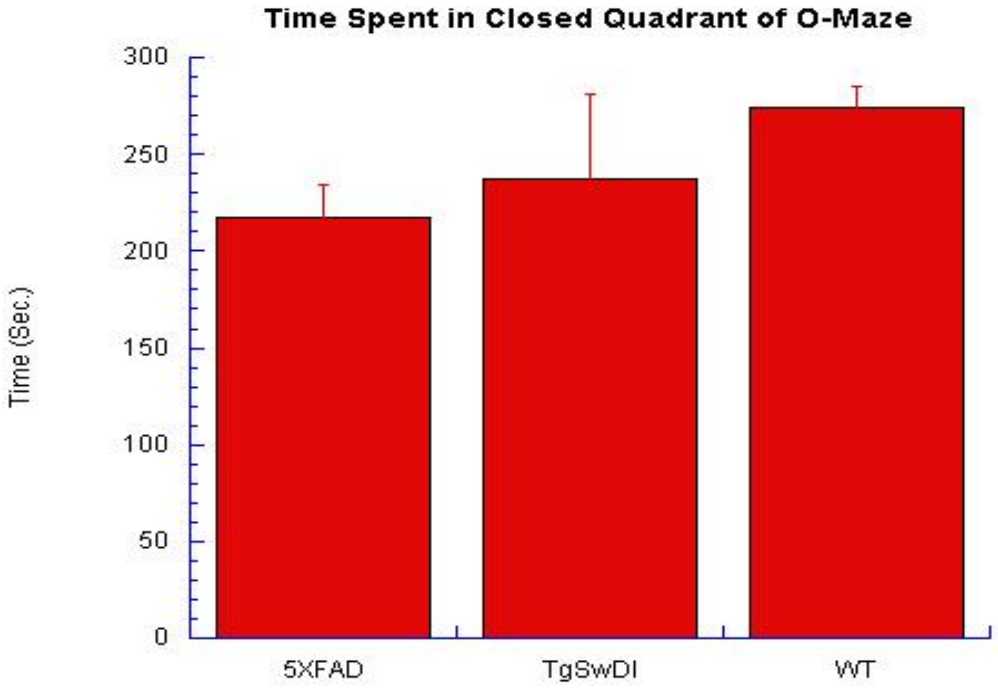
Time Spent in Closed Quadrant of O-Maze
Time (Sec.)
300
250
200
150
100
50
0
5XFAD
TgSwDI
WT

f)

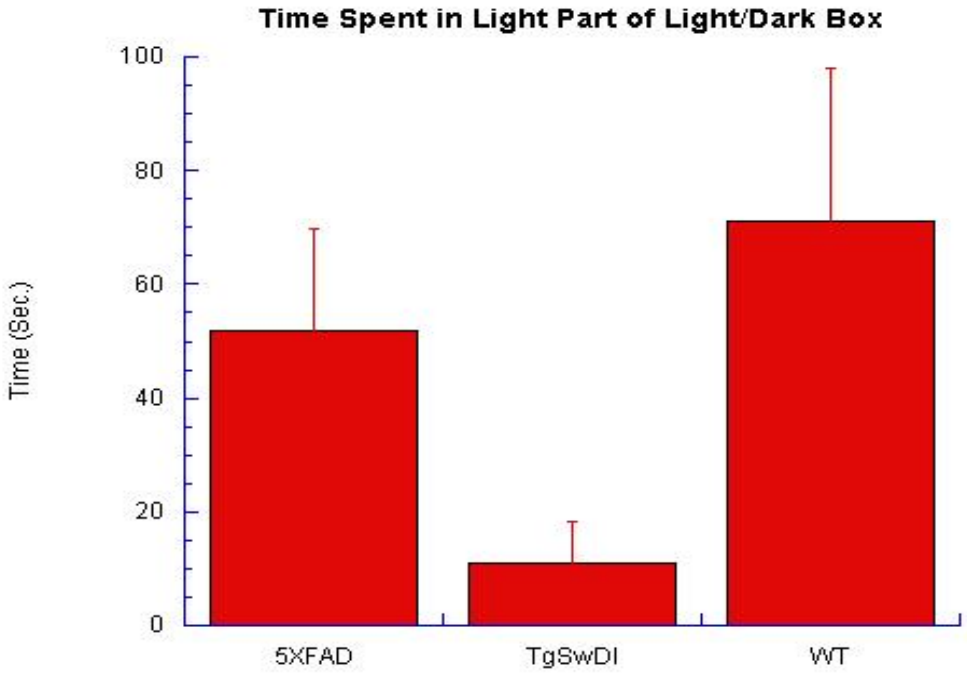
Time Spent in Light Part of Light/Dark Box
Time (Sec.)
100
80
60
40
20
0
5XFAD
TgSwDI
WT

g)

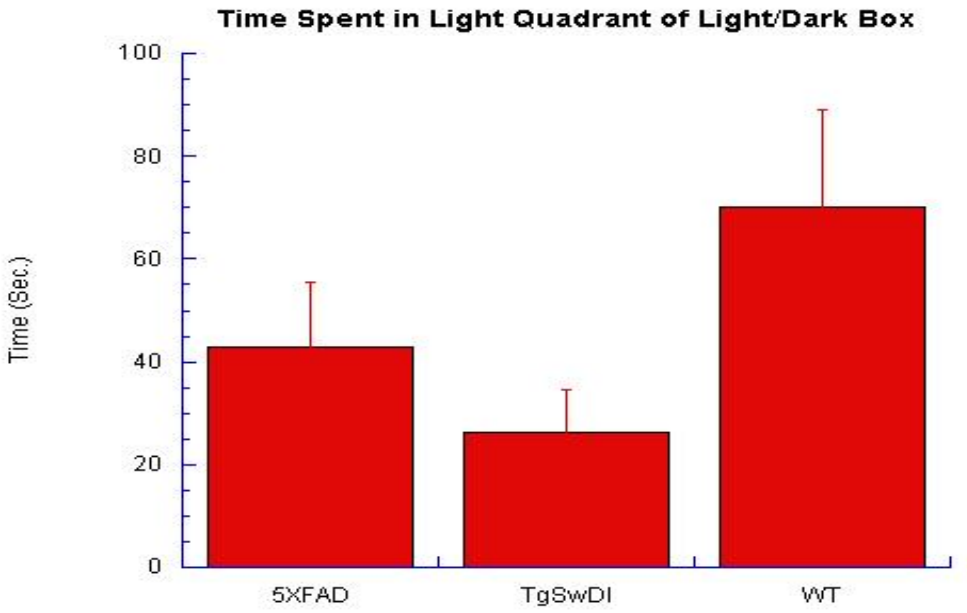
Time Spent in Light Quadrant of Light/Dark Box
Time (Sec.)
100
80
60
40
20
0
5XFAD
TgSwDI
WT

h)

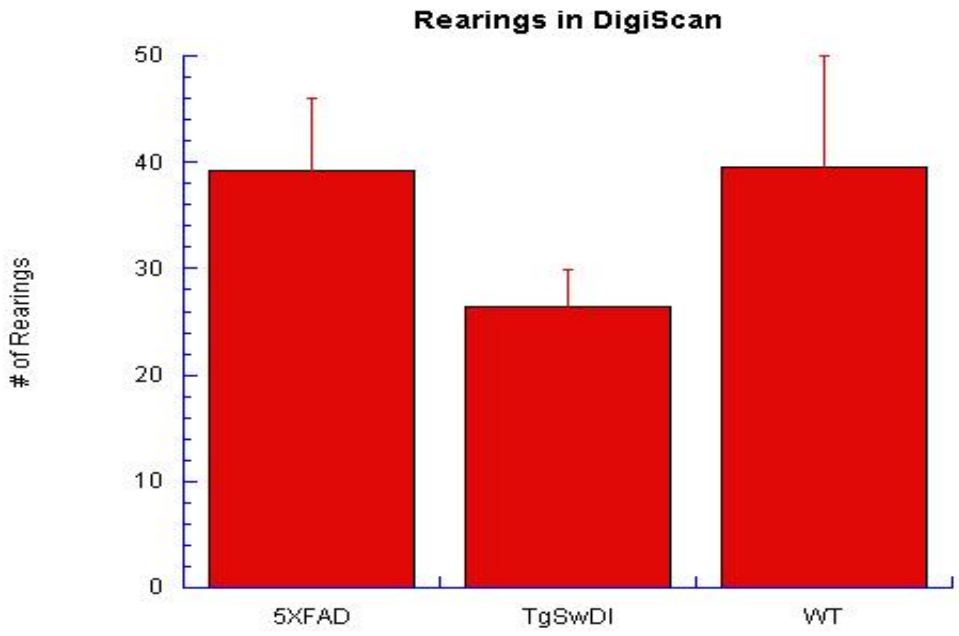
Rearings in DigiScan
# of Rearings
50
40
30
20
10
0
5XFAD
TgSwDI
WT

i)

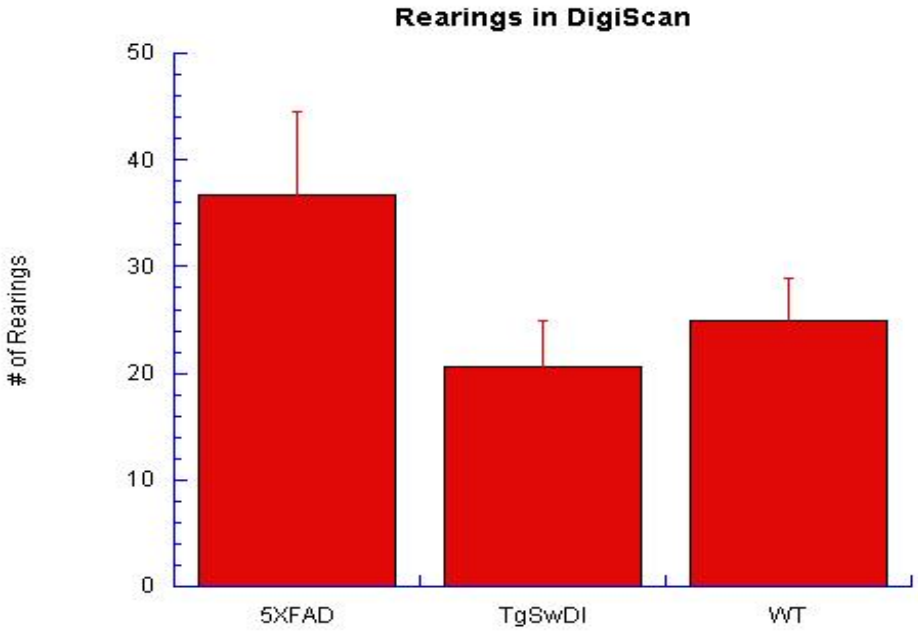
Rearings in DigiScan
# of Rearings
50
40
30
20
10
0
5XFAD
TgSwDI
WT

j)

Figure 4

Graph showing 3 (a) and 6 month (b) 5XFAD, TgSwDI, and WT animal performance on the latency to find measure in the Barnes maze spatial working/reference memory task. 3-month old wild type (Wild-Type 3), 6-month old wild type (Wild-Type 6), 3-month old TgSwDI (TgSwDI 3), 6-month old TgSwDI (TgSwDI 6), 3-month old 5XFAD (5XFAD 3), 6-month old 5XFAD (5XFAD 6). At 3 months, TgSwDI animals show impairment relative to age-matched wild-type controls and 5XFAD animals ($p<.05$). There is no significant difference between 5XFAD and wild-type animal performance at this early time point. At 6 months, TgSwDI and 5XFAD animals were comparably impaired and both showed significant deficits compared to age-matched wild-type controls ($p<.05$). Error bars represent SEM.

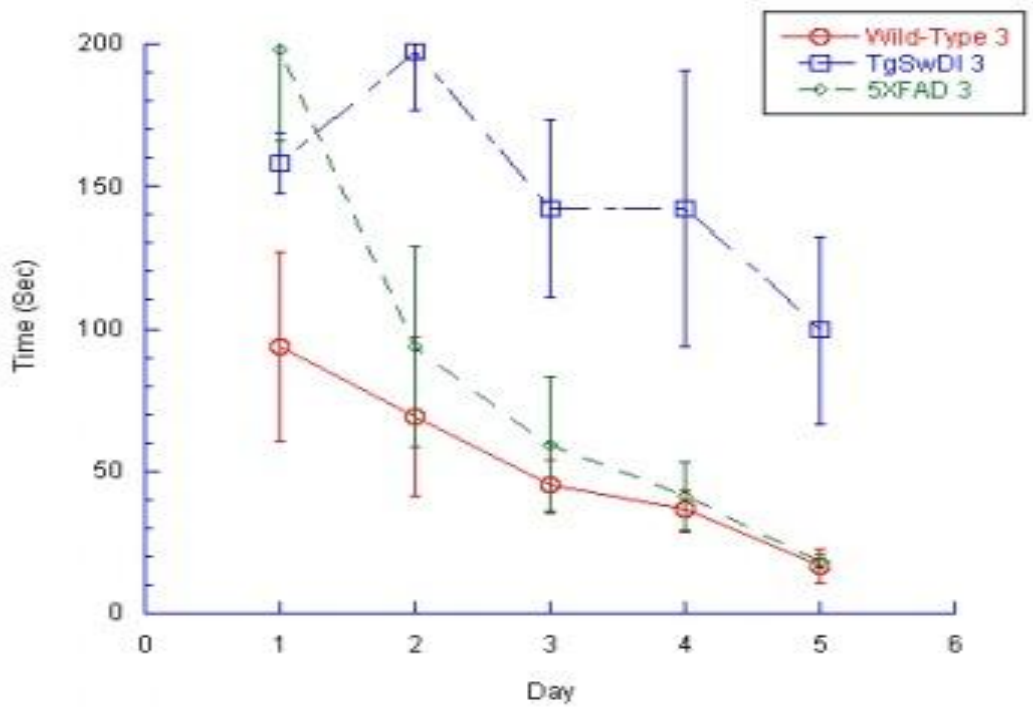

a)

b)

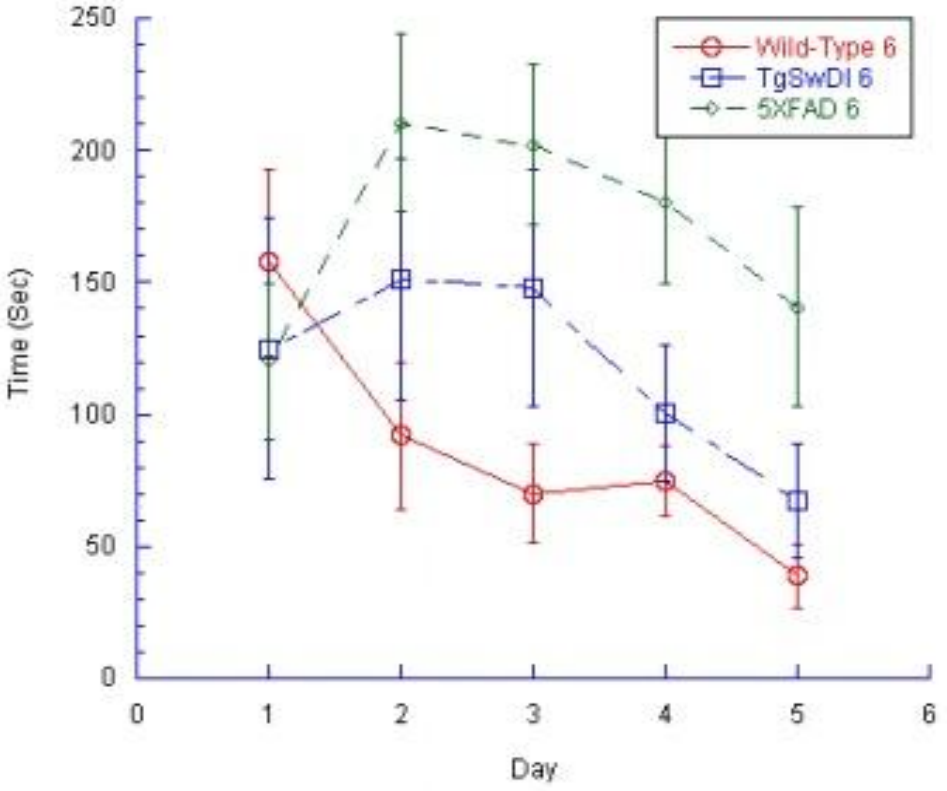
Wild-Type 6
TgSwDI 6
5XFAD 6
Time (Sec)
Day
0
50
100
150
200
250
0
1
2
3
4
5
6

Figure 5

Rabbit polyclonal 1-28 anti-amyloid with anti-rabbit IgG 488 immunoflourescence stain for Aβ40 and Aβ42 species in subiculum of 3 month old a) 5XFAD vs. b) TgSwDI and 6 month old c) 5XFAD vs. d) TgSwDI animals. Note the pattern of deposition of Aβ in the subiculum of the 5XFAD as dense, brightly stained individual circular cores compared to in the TgSwDI as lightly stained, continuous patches. Scale bar represents 200μm.

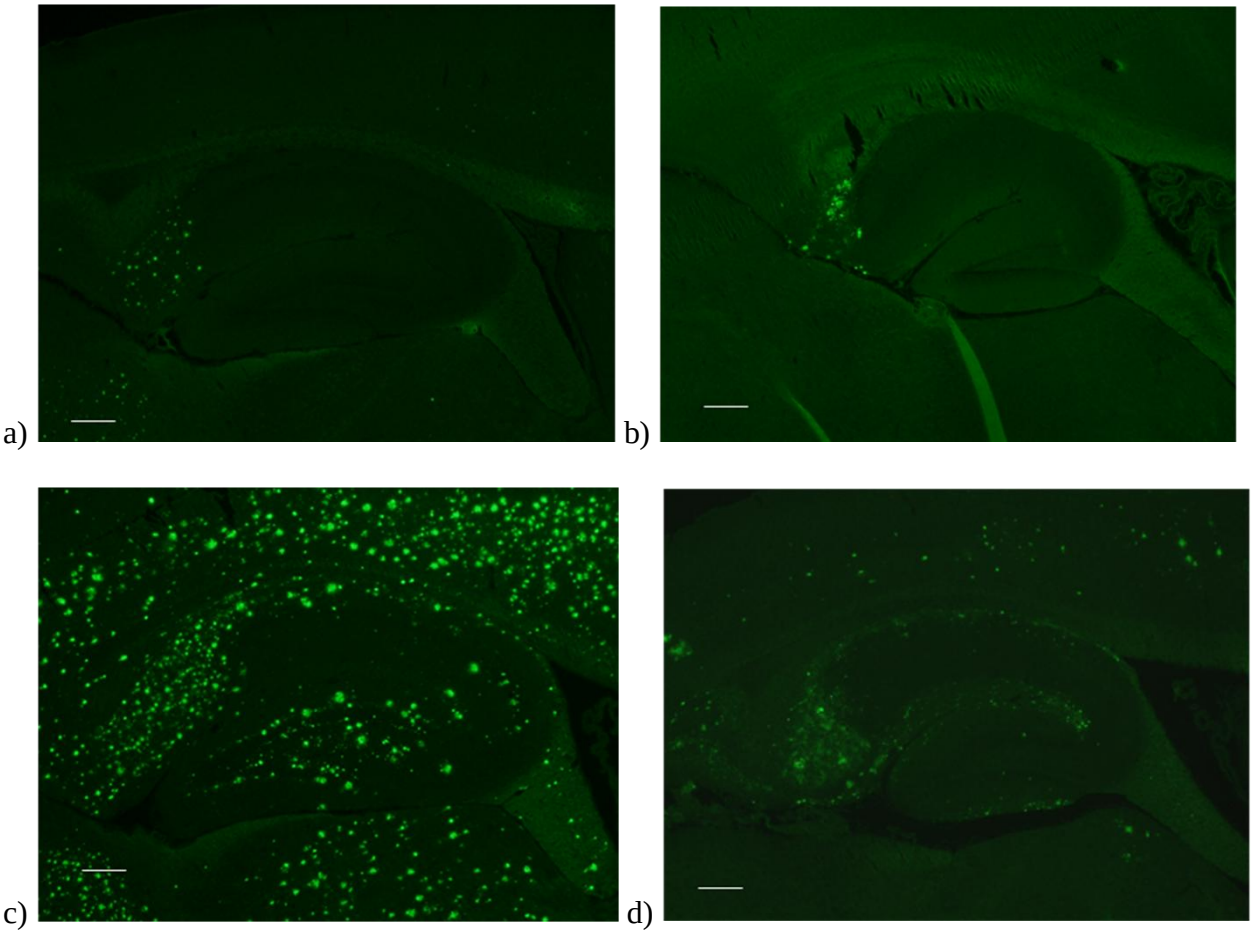

Figure 6

Scatterplot representation of rank data from immunohistochemical/immunoflourescence staining. 3 and 6 month data of a & b) % Microvessels associated with amyloid, c & d) Area fraction of Total Aβ40 and Aβ42, and e & f) microglia density. 5XFAD animals are represented in blue and TgSwDI animals are in red.

a)

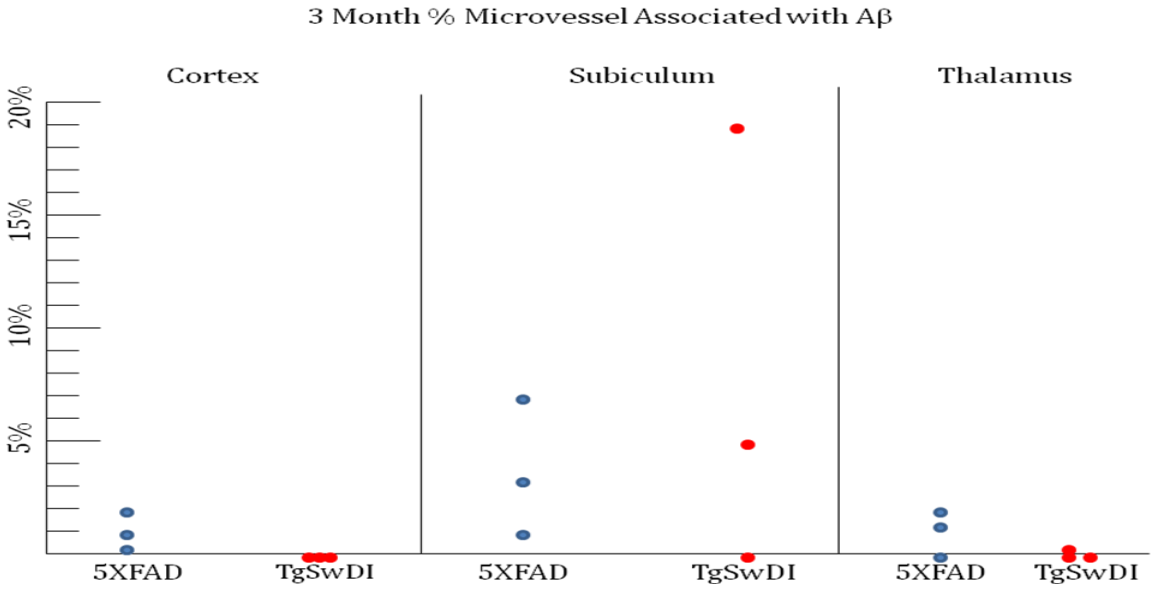

b)

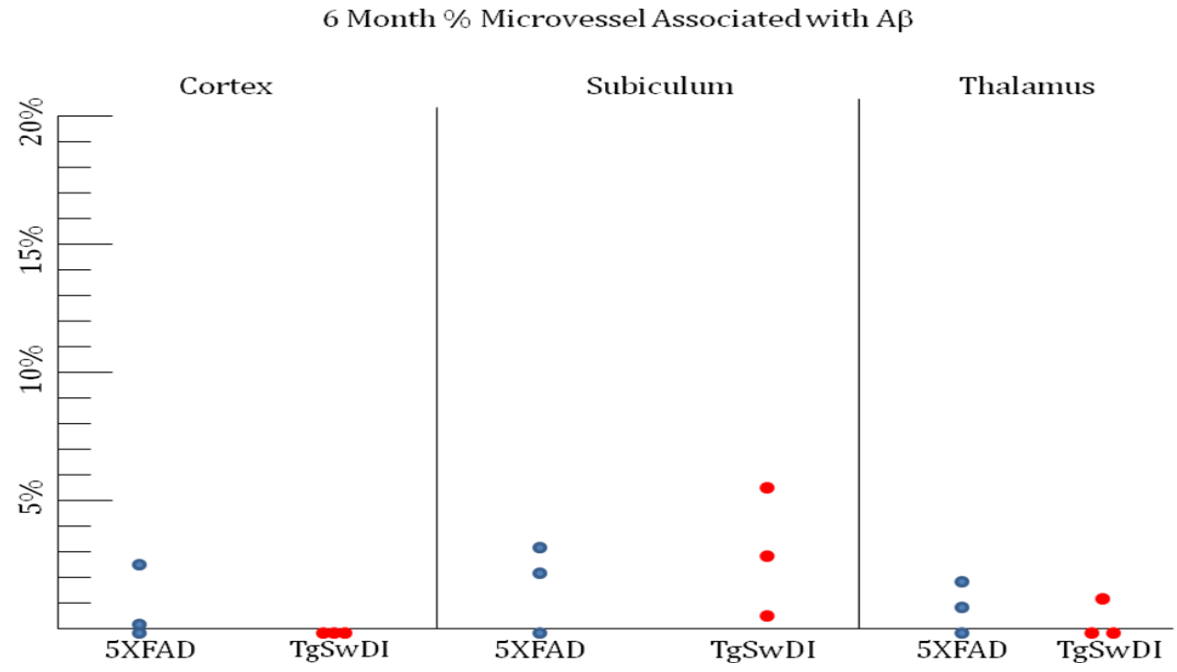

c)

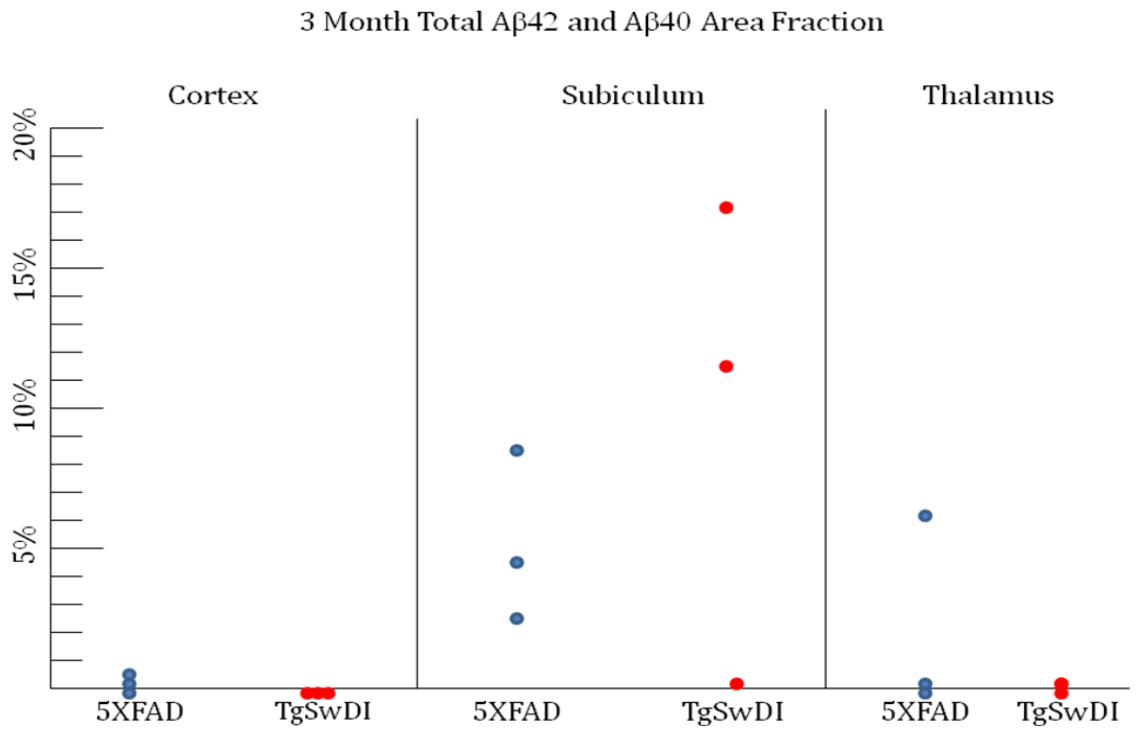
3 Month Total Aβ42 and Aβ40 Area Fraction
Cortex
Subiculum
Thalamus
20%
15%
10%
5%
5XFAD
TgSwDI
5XFAD
TgSwDI
5XFAD
TgSwDI

d)

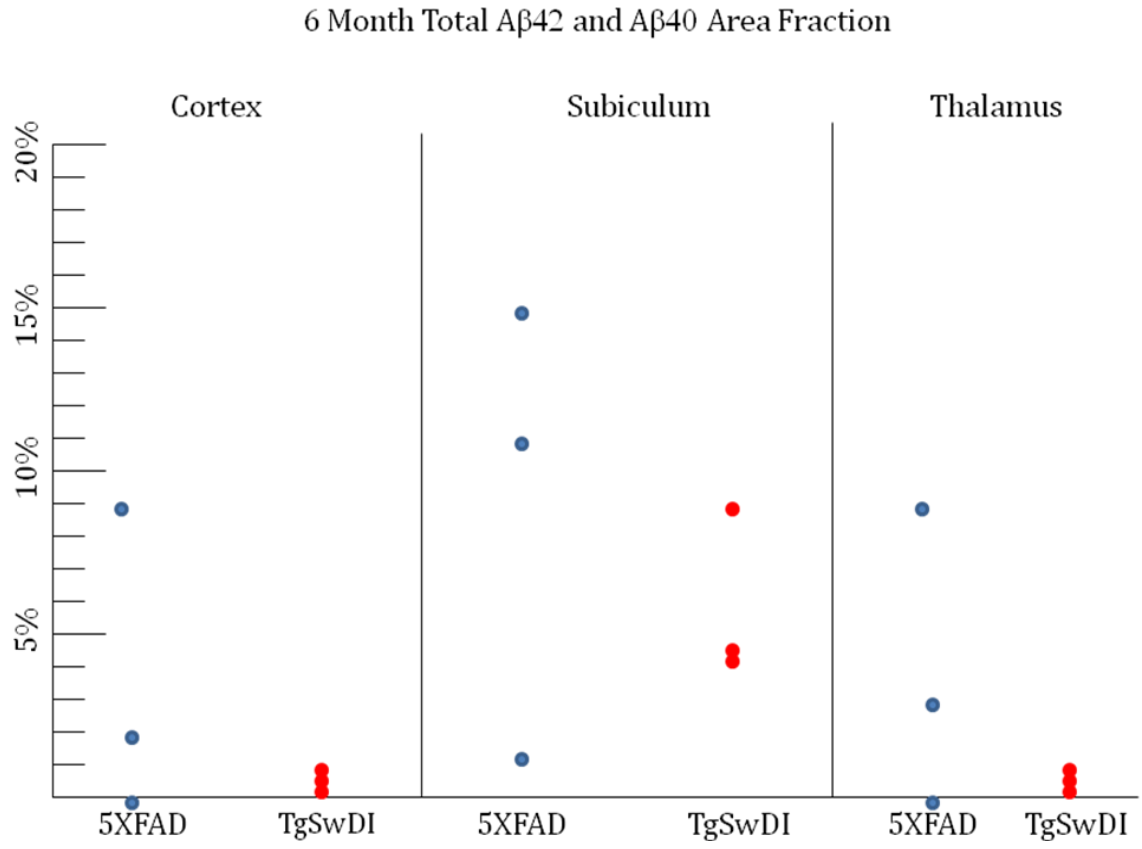
6 Month Total Aβ42 and Aβ40 Area Fraction
Cortex
Subiculum
Thalamus
20%
15%
10%
5%
5XFAD
TgSwDI
5XFAD
TgSwDI
5XFAD
TgSwDI

e)

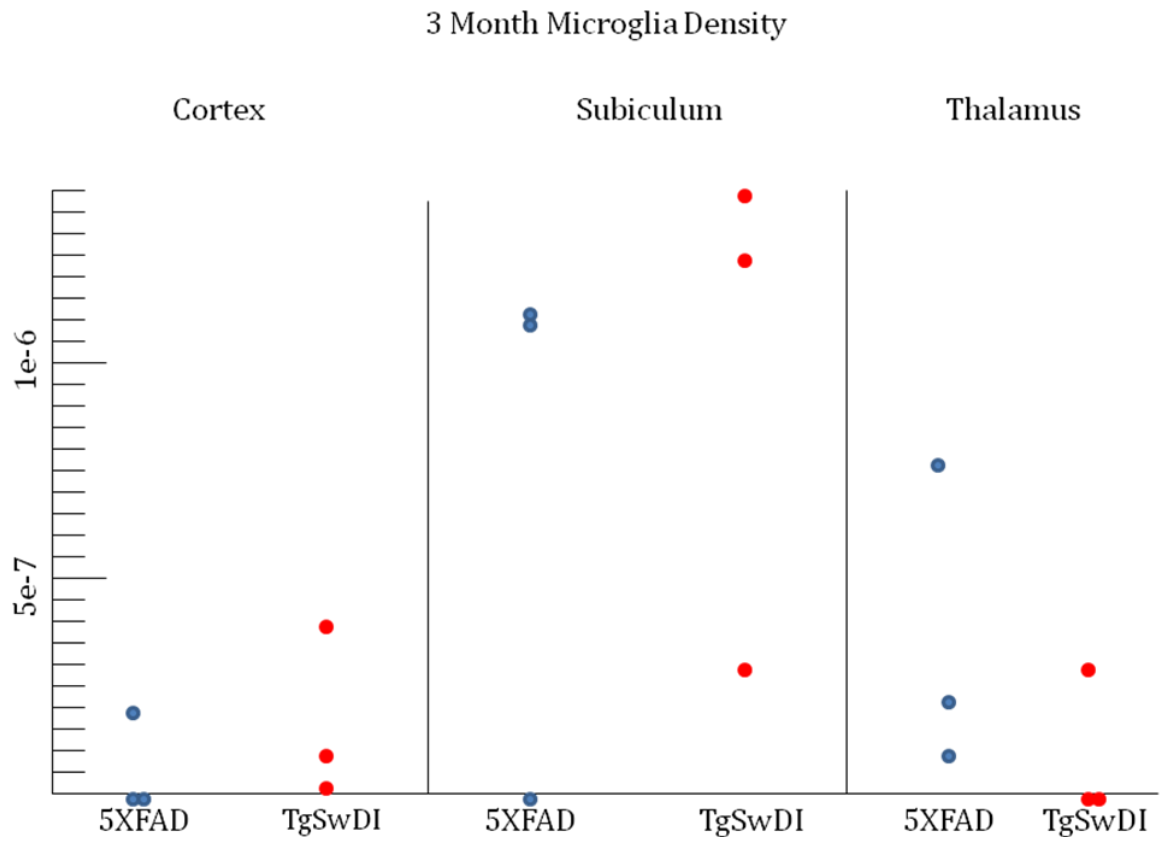
3 Month Microglia Density
Cortex
Subiculum
Thalamus
1e-6
5e-7
5XFAD
TgSwDI
5XFAD
TgSwDI
5XFAD
TgSwDI

f)

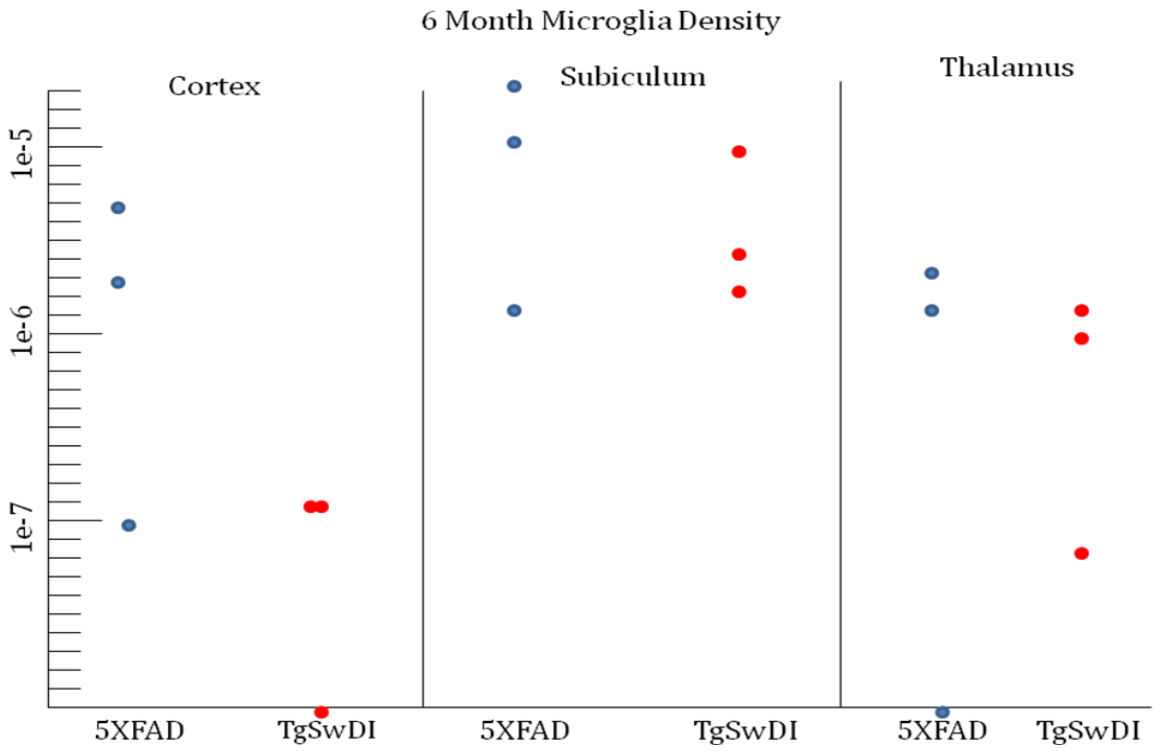
6 Month Microglia Density
Cortex
Subiculum
Thalamus
1e-5
1e-6
1e-7
5XFAD
TgSwDI
5XFAD
TgSwDI
5XFAD
TgSwDI

Appendix B

Table 1. Correlation matrix of different Aβ species with each other

	Aβ42S	Aβ42I	Aβ40S	Aβ40I
Aβ42S	1.00	.86	.73	.95
Aβ42I	.86	1.00	.93	.82
Aβ40S	.73	.93	1.00	.69
Aβ40I	.952	.82	.69	1.00

Table 2. Results of immunhistochemical/immunoflourescence staining and stereological quantification for a) 3 month age group, b) 6 month age group. Total Aβ ELISA measured in pg/mg, total Aβ40/42 measured in percentage of total area stained both dense core and (spray pattern), activated microglia measured in density/μ^3 . Rank in Barnes maze learning from 1/# (best, steepest learning curve) to #/# (worst, flattest learning curve). Percentage of microvessels associated with Aβ42 fibrillary plaque (% Vessels), Subiculum (Sub.), Thalamus (Thal.), Microglial activation (Microglia)

a)

Genotype	Animal #	Total Aβ ELISA	% Vessels (Cortex)	% Vessels (Sub.)	% Vessels (Thal.)	Total Aβ40/42 (Cortex)	Total Aβ40/42 (Sub.)	Total Aβ40/42 (Thal.)
5XFAD	101	25156	1.8	3.1	1.5	0.24 (.49)	3.81 (8.43)	0.32 (6.17)
	102	23218	0.8	6.8	1.8	0.07 (0.21)	2.29 (2.29)	0.19 (0.34)
	91	101.52	0.2	0.9	0	0.05 (0.08)	2.38 (4.5)	0 (0)
TgSwDI	157	2155	0	18.5	0.4	0 (0.01)	4.1 (11.42)	0 (0.12)
	158	1171	0	4.8	0	0 (0)	5.52 (17.3)	0.04 (0.16)
	159	131	0	0	0	0 (0)	0.07 (0.19)	0 (0)

Animal #	Microglia (Cortex)	Microglia (Sub.)	Microglia (Thal.)	Rank in Barnes Learning
101	0	2.27e-6	7.87e-7	5/6
102	2.27e-7	2.23e-6	1.98e-7	6/6
91	0	0	1.07e-7	1/6
157	1.04e-7	5.28e-6	0	2/7
158	4.92e-7	3.58e-6	0	7/7
159	0	3.1e-7	3.0e-7	3/7

b)

Genotype	Animal #	Total Aβ ELISA	% Vessels (Cortex)	% Vessels (Sub.)	% Vessels (Thal.)	Total Aβ40/42 (Cortex)	Total Aβ40/42 (Sub.)	Total Aβ40/42 (Thal.)
5XFAD	43	217302	2.4	3.1	1.9	7.53 (8.77)	7.17 (15.1)	4.79 (8.51)
	46	4960	0.3	1.9	1.2	2.69 (2.05)	6.68 (11.22)	1.9 (2.98)
	68	2701	0	0	0	0 (0)	0.4 (1.08)	0 (0)
TgSwDI	53	7174	0	5.4	1.5	0.34 (0.98)	1.37 (4.02)	0.45 (0.94)
	55	2808	0	2.8	0	0.13 (0.3)	1.2 (4.13)	0.05 (0.09)
	52	72	0	0.7	0	0.29 (0.73)	1.37 (8.77)	0.3 (0.58)

Animal #	Microglia (Cortex)	Microglia (Sub.)	Microglia (Thal.)	Rank in Latency to Find
43	8.82e-6	5.0e-5	3.65e-6	5/7
46	3.23e-6	1.0e-5	2.33e-6	4/7
68	1.11e-7	2.48e-6	0	1/7
53	2.31e-7	1e-5	2.37e-6	4/6
55	0	3.56e-6	8.78e-8	6/6
52	2.24e-7	5.32e-6	1.58e-6	2/6